

# Integrability and linear stability of nonlinear waves

Antonio Degasperis

Dipartimento di Fisica, “Sapienza” Università di Roma, Italy

E-mail: antonio.degasperis@uniroma1.it

Sara Lombardo

Department of Mathematics, Physics and Electrical Engineering

Northumbria University, Newcastle upon Tyne, UK

E-mail: sara.lombardo@northumbria.ac.uk

Matteo Sommacal

Department of Mathematics, Physics and Electrical Engineering

Northumbria University, Newcastle upon Tyne, UK

E-mail: matteo.sommacal@northumbria.ac.uk

January 27, 2023

## Abstract

It is well known that the linear stability of solutions of partial differential equations which are integrable can be very efficiently investigated by means of spectral methods.

We present here a direct construction of the eigenmodes of the linearized equation by using only their associated Lax pair with no reference to spectral data and boundary conditions. This local construction is given in the general  $N \times N$  matrix scheme so as to be applicable to a large class of integrable equations, including the multicomponent nonlinear Schrödinger system and the multi-wave resonant interaction system.

The analytical and numerical computations involved in this general approach are detailed as an example for  $N = 3$  for the particular system of two coupled nonlinear Schrödinger equations in the defocusing, focusing and mixed regimes. The instabilities of the continuous wave solutions are fully discussed in the entire parameter space of their amplitudes and wave numbers. By defining and computing the spectrum in the complex plane of the spectral variable, the eigenfrequencies are explicitly expressed. According to their topological properties, the complete classification of these spectra in the parameter space is presented and graphically displayed. The continuous wave solutions are linearly unstable for a generic choice of the coupling constants.

Keywords: Nonlinear Waves, Integrable Systems, Wave Coupling, Resonant Interactions, Modulational Instability, Coupled Nonlinear Schrödinger equations

# 1 Introduction

The problem of stability is central to the entire field of nonlinear wave propagation and is a fairly broad subject. Here we are specifically concerned with the early stage of amplitude modulation instabilities due to quadratic and cubic nonlinearities and we consider in particular dispersive propagation in a one dimensional space, or diffraction in a two dimensional space.

After the first observations of wave instability [7, 38, 39] (see also *e.g.* [50]), the research on this subject has grown very rapidly because similar phenomena appear in various contexts such as water waves [47], optics [5], Bose-Einstein condensation [26] and plasma physics [27]. Experimental findings were soon followed by theoretical and computational works. Predictions regarding short time evolution of small perturbations of the initial profile can be obtained by standard linear stability methods, see *e.g.* [41] and references therein. Very schematically, if  $u(x, t)$  is a particular solution of the wave equation evolving in time  $t$ , and if  $u + \delta u$  is the perturbed solution of the same equation, then, at the first order of approximation,  $\delta u$  satisfies a linear equation with non-constant coefficients. Solving the initial value problem  $\delta u(x, 0) \rightarrow \delta u(x, t)$  in general is not tractable by analytic methods. It is only for special solutions  $u(x, t)$ , such as nonlinear plane waves or solitary localized waves, see *e.g.* [41], that this initial value problem can be approached by solving an eigenvalue problem for an ordinary differential operator in the space variable  $x$ . In this way the computational task reduces to constructing the eigenmodes while the corresponding eigenvalues are simply related to the proper frequencies. For very special solutions this procedure exceptionally leads to solve the initial value problem for the linearized equation via Fourier analysis: a simple and well known example of this case is the linearization of the focusing Non Linear Schrödinger (NLS) equation  $iu_t + u_{xx} + 2|u|^2u = 0$  around its Continuous Wave (CW) solution  $u(x, t) = e^{2it}$ . Here and thereafter subscripts  $x$  and  $t$  denote partial differentiation, unless differently specified. The computation of all the eigenfrequencies yields the relevant information about the stability of  $u(x, t)$  provided the set of eigenmodes be complete in the functional space characterized by the boundary conditions satisfied by the initial perturbation  $\delta u(x, 0)$ . Since the main step of this method is that of finding the spectrum of a differential operator, the stability property of the solution  $u(x, t)$  is also referred to as *spectral stability*. It is clear that this method applies to a limited class of solutions of the wave equation.

An alternative and more powerful approach to stability has been introduced [3] shortly after the discovery of the spectral method to solve the Kortewg-de Vries (KdV) and NLS equations (*e.g.*, see the textbooks [4, 10, 34]). This method originates from the representation of the perturbation  $\delta u(x, t)$  in terms of the so-called “squared eigenfunctions” (see below). Its evident drawback is that its applicability is limited to the very special class of integrable wave propagation equations. Notwithstanding this condition, it remains of important practical interest because several integrable partial differential equations have been derived in various physical contexts as reliable, though approximate, models [19, 4, 12]. Moreover, the stability properties of particular solutions of an integrable wave equation provide a strong insight about similar solutions of a different non-integrable, but just close enough, equation. Among the many properties defining the concept of integrability the one that we consider here is the existence of a Lax pair of two linear ordinary differential

equations, one in the space variable  $x$  and the other in the time variable  $t$  (see next Section). Thus a spectral problem with respect to the variable  $x$  already appears at the very beginning of the integrability scheme. With appropriate specifications, as stated below, this observation leads to the construction of the eigenmodes of the linearized equation, in terms of the solutions of the Lax pair. Moreover, in this way one is able to compute the corresponding eigenfrequencies which give the necessary and sufficient information to assess linear stability. Explicit expressions of such eigenmodes have been obtained if the unperturbed wave amplitude  $u$  is a cnoidal wave (*e.g.* see [28, 40, 30] for the KdV equation and [29] for the NLS equation), or if it is a soliton solution [43] or an arbitrary solution [44]. Therefore the computational strategy amounts to constructing the set of eigenmodes and eigenfrequencies. It should be pointed out that the integrability methods, in an appropriate functional space of the solutions, provide also the way of deriving the closure and completeness relations of the eigenmodes, see *e.g.* [24, 43, 44] for solutions which vanish sufficiently fast as  $|x| \rightarrow 0$ . In this respect, a word of warning is appropriate. The boundary conditions imposed on the solutions  $u(x, t)$  play a crucial role in proving that the wave equation is integrable. Thus, in particular for the NLS equation, integrability methods have been applied so far to linear stability of wave solutions which, as  $|x| \rightarrow \infty$ , either vanish as localized soliton [43], or go to a CW solution (see the lecture notes [16]), or else are periodic,  $u(x, t) = u(x + L, t)$  [9]. In these cases to any solution  $u(x, t)$  one can associate a set of spectral data, the spectral transform, say the analog of the Fourier transform in a nonlinear context. This correspondence allows to solve the initial value problem of the wave equation. As a byproduct, this formalism yields also a spectral representation of the small perturbations  $\delta u(x, t)$  in terms of the corresponding small change of the spectral data. This connection is given by the squared eigenfunctions (see [3, 24, 46] for the NLS equation, and [10] for the KdV equation) which play the role of the Fourier exponentials. Indeed the squared eigenfunctions, which are computed by solving the Lax pair, are the eigenmodes of the linearized equation for  $\delta u(x, t)$ . More than this, integrability allows to go beyond the linear stage of the evolution of small perturbations. This is possible by the spectral method of solving the initial value problem for the perturbed solution  $u + \delta u$  which therefore yields the long time evolution of  $\delta u$  beyond the linear approximation, see for instance [48, 8]. However, this important problem falls outside the scope of the present work and it will not be considered here.

The stability conditions of a given solution  $u(x, t)$  may depend on parameters. They come from the coefficients of the wave equation, and from the parameters (if any) which characterize the solution itself. This obvious observation implies that there may be thresholds in the parameter space. The investigation of such thresholds is rather simple when dealing with scalar (one-component) waves. For instance, the KdV equation has no frozen coefficients, for a simple rescaling can set them equal to any real number, so that it reads  $u_t + u_{xxx} + uu_x = 0$ . On the other hand, after rescaling, the NLS equation comes with a sign in front of the cubic term, distinguishing between defocusing and focusing self-interaction. These two different versions of the NLS equation lead to different phenomena such as modulation stability and instability of the continuous wave solution (for an introductory review, see [16]). Wave propagation equations which model different physical systems may have more structural coefficients whose values cannot be simultaneously, and independently, rescaled. This is the case when two or more waves resonate and propagate while coupling to each other. In this case, the wave equations do not happen to be integrable for all choices of the coefficients. A well known example, which is in fact the main

focus of this work, is that of two interacting fields,  $u_j$ ,  $j = 1, 2$ , which evolve according to the coupled system of NLS equations

$$iu_{jt} + u_{jxx} - 2(s_1|u_1|^2 + s_2|u_2|^2)u_j = 0, \quad j = 1, 2 \quad (1)$$

where  $(s_1|u_1|^2 + s_2|u_2|^2)$  is the self- and cross-interaction term. This is integrable only in three cases [49], namely (after appropriate rescaling):  $s_1 = s_2 = 1$  (defocusing Manakov model),  $s_1 = s_2 = -1$  (focusing Manakov model) [32], and the mixed case  $s_1 = -s_2 = 1$ . These three integrable systems of two Coupled NLS (CNLS) equations are of interest in few special applications (*e.g.* [33, 20, 42, 35]), while in various contexts (*e.g.* in optics [5] and in fluid dynamics [47, 2]), the coupling constants  $s_1, s_2$  take different values and the CNLS system happens to be non-integrable. Yet the analysis of the three integrable cases is still relevant in the study of the (sufficiently close) non-integrable ones [45]. The linear stability of CW solutions of integrable CNLS systems have been investigated by means of the Fourier transform [21] and by spectral methods [31] to mainly show that instability may occur also in defocusing media, in contrast to scalar waves which are modulationally unstable only in the focusing case. In the following we use the integrability methods to compute the spectrum of the CW solution in the parameter space of the two amplitudes and coupling constants. Depending on the value of the parameters the spectrum changes and so the linear stability properties. Our investigation is completed by a classification of spectra according to their topological features.

This article is organised as follows. In the next section (Section 2) we give the general expression of the eigenmodes of the linearized equation for the general  $N \times N$  matrix scheme so as to capture a large class of integrable systems. There we define the  $x$ -spectrum in the complex plane of the spectral variable. In Section 3 we provide an example of application of the theory by specializing the formalism introduced in Section 2 to deal with the CNLS equations. We characterize the  $x$ -spectrum in the complex plane of the spectral variable and classify its properties. Section 3.3 is devoted to discussing the classification of spectra in terms of the physical parameters while a brief conclusion with perspective of future work is the content of Section 4. Details regarding computational and numerical aspects of the problem are confined in Appendices.

## 2 Integrable wave equations and small perturbations

The integrable partial differential equations (PDEs) which are considered here are associated with the following pair of matrix ordinary differential equations (ODEs), also known as *Lax pair* (*e.g.*, see [10, 34, 1]),

$$\Psi_x = X\Psi, \quad \Psi_t = T\Psi, \quad (2)$$

where  $\Psi$ ,  $X$  and  $T$  are  $N \times N$  matrix-valued complex functions. The existence of a fundamental (*i.e.* non singular) matrix solution  $\Psi = \Psi(x, t)$  of this overdetermined system is guaranteed by the condition that the two matrices  $X$  and  $T$  satisfy the differential equation

$$X_t - T_x + [X, T] = 0. \quad (3)$$

We recall here that, unless differently specified, a subscripted variable means partial differentiation with respect to that variable, and  $[A, B]$  stands for the commutator  $AB - BA$ .

In order to identify this condition (3) as an integrable partial differential equation for some of the entries of the matrix  $X$ , it is essential that both matrices  $X$  and  $T$  parametrically depend on an additional complex variable  $\lambda$ , known as the *spectral parameter*. In order to make this introductory presentation as simple as possible, we assume that  $X(\lambda)$  and  $T(\lambda)$  be polynomial in  $\lambda$  with degrees  $n$  and  $m$ , respectively. As a consequence, the matrix  $X_t - T_x + [X, T]$  is as well polynomial in  $\lambda$  with degree  $n + m$  and therefore the compatibility equation (3) yields  $n + m + 1$  equations for the matrix coefficients of the polynomials  $X$  and  $T$ .

If the pair  $X$  and  $T$  is a given solution of (3), we consider a new solution  $X \rightarrow X + \delta X$ ,  $T \rightarrow T + \delta T$ , which differs by a small change of the matrices  $X$  and  $T$ , with the implication that the pair of matrices  $\delta X$  and  $\delta T$ , at the first order in this small change, satisfy the *linearized equation*

$$(\delta X)_t - (\delta T)_x + [\delta X, T] + [X, \delta T] = 0. \quad (4)$$

Again the left-hand side of this linearized equation has a polynomial dependence on  $\lambda$  and the vanishing of all its coefficients results in a number of algebraic or differential equations. These obvious observations lead us to focus on the matrix linearized equation (4) itself, which reads, by setting  $A = \delta X$ ,  $B = \delta T$ ,

$$A_t - B_x + [A, T] + [X, B] = 0, \quad (5)$$

and to search for its solutions  $A(x, t, \lambda)$  and  $B(x, t, \lambda)$ . Our main target is to find those solutions which are related to the fundamental matrix solution  $\Psi(x, t, \lambda)$  of the Lax pair (2). To this purpose we first note that the similarity transformation

$$M(\lambda) \rightarrow \Phi(x, t, \lambda) = \Psi(x, t, \lambda) M(\lambda) \Psi^{-1}(x, t, \lambda), \quad (6)$$

of a constant (*i.e.*  $x, t$ -independent) matrix  $M(\lambda)$  yields the transformed matrix  $\Phi$  which, for any given arbitrary matrix  $M$ , satisfies the pair of linear ODEs

$$\Phi_x = [X, \Phi], \quad \Phi_t = [T, \Phi]. \quad (7)$$

Equations (7) are compatible with each other because of (3). Then, for future reference, we point out the following observations.

**Proposition 1** *If the pair  $A, B$  solves the linearized equation (5) then also the pair*

$$F = [A, \Phi], \quad G = [B, \Phi] \quad (8)$$

*is a solution of the same linearized equation (5), namely*

$$F_t - G_x + [F, T] + [X, G] = 0. \quad (9)$$

This is a strait consequence of the Jacobi identity and of the assumption that the matrix  $\Phi$  be a solution of (7).

**Proposition 2** *The following expressions*

$$F = \left[ \frac{\partial X}{\partial \lambda}, \Phi \right], \quad G = \left[ \frac{\partial T}{\partial \lambda}, \Phi \right] \quad (10)$$

*provide a solution of the linearized equation (9).*

The validity of this statement follows from the fact that the matrices

$$A = \frac{\partial X}{\partial \lambda}, \quad B = \frac{\partial T}{\partial \lambda}, \quad (11)$$

obviously solve the linearized equation (5), and from Proposition 1.

At this point we go back to the nonlinear matrix PDE which follows from the condition (3). In view of the applications within the theory of nonlinear resonant phenomena that we have in mind (which include the multicomponent nonlinear Schrödinger system and the multi-wave resonant interaction system), we assume that the polynomials  $X(\lambda)$  and  $T(\lambda)$ , see (2), have degree one and, respectively, two, namely

$$X(\lambda) = i\lambda\Sigma + Q, \quad T(\lambda) = \lambda^2 T_2 + \lambda T_1 + T_0. \quad (12)$$

where  $\Sigma$ ,  $Q$ ,  $T_0$ ,  $T_1$  and  $T_2$  are matrix-valued functions of  $x$  and  $t$ . The extension to higher degree polynomials results only in an increased computational effort.

Moreover, before proceeding further, few preliminary observations and technicalities are required. First, we assume that the  $N \times N$  matrix  $\Sigma$ , see (12), be constant and Hermitian. Therefore, without any loss of generality,  $\Sigma$  is set to be diagonal and real, namely, in block-diagonal notation,

$$\Sigma = \text{diag}\{\alpha_1 \mathbb{1}_1, \dots, \alpha_L \mathbb{1}_L\}, \quad 2 \leq L \leq N, \quad (13)$$

where the real eigenvalues  $\alpha_j$ ,  $j = 1, \dots, L$ , satisfy  $\alpha_j \neq \alpha_k$  if  $j \neq k$ , while  $\mathbb{1}_j$  is the  $n_j \times n_j$  identity matrix where  $n_j$  is the (algebraic) multiplicity of the eigenvalue  $\alpha_j$ . Of course,  $\sum_{j=1}^L n_j = N$ . Note that this matrix  $\Sigma$  induces the splitting of the set of  $N \times N$  matrices into two subspaces, namely that of *block-diagonal* matrices and that of *block-off-diagonal* matrices. Precisely, if  $\mathcal{M}$  is any  $N \times N$  matrix, then we adopt the following notation

$$\mathcal{M} = \mathcal{M}^{(d)} + \mathcal{M}^{(o)}, \quad (14)$$

where

$$\mathcal{M}^{(d)} = \begin{pmatrix} \boxed{n_1 \times n_1} & 0 & 0 & 0 & 0 \\ 0 & \boxed{\cdot} & 0 & 0 & 0 \\ 0 & 0 & \boxed{\cdot} & 0 & 0 \\ 0 & 0 & 0 & \boxed{\cdot} & 0 \\ 0 & 0 & 0 & 0 & \boxed{n_L \times n_L} \end{pmatrix} \quad (15a)$$

is the block-diagonal part of  $\mathcal{M}$ , and

$$\mathcal{M}^{(o)} = \begin{pmatrix} 0 & \boxed{n_1 \times n_2} & \boxed{\cdot} & \boxed{\cdot} & \boxed{n_1 \times n_L} \\ \boxed{n_2 \times n_1} & 0 & \boxed{\cdot} & \boxed{\cdot} & \boxed{\cdot} \\ \boxed{\cdot} & \boxed{\cdot} & 0 & \boxed{\cdot} & \boxed{\cdot} \\ \boxed{\cdot} & \boxed{\cdot} & \boxed{\cdot} & 0 & \boxed{\cdot} \\ \boxed{n_L \times n_1} & \boxed{\cdot} & \boxed{\cdot} & \boxed{\cdot} & 0 \end{pmatrix} \quad (15b)$$

is its block-off-diagonal part. Consistently with this notation, the entries  $\mathcal{M}_{jk}$  of an  $N \times N$  matrix  $\mathcal{M}$  are meant to be matrices themselves of dimension  $n_j \times n_k$  with the implication that the “matrix elements”  $\mathcal{M}_{jk}$  may not commute with each other (*i.e.* the subalgebra of block-diagonal matrices, see (15a), is non-commutative). Moreover, one should keep

in mind that the off-diagonal entries  $\mathcal{M}_{jk}$  are generically rectangular. We also note that the product of two generic  $N \times N$  matrices  $\mathcal{A}$  and  $\mathcal{B}$  follows the rules:  $(\mathcal{A}^{(d)} \mathcal{B}^{(d)})^{(o)} = 0$ ,  $(\mathcal{A}^{(d)} \mathcal{B}^{(o)})^{(d)} = 0$  while, for  $N > 2$ , the product  $\mathcal{A}^{(o)} \mathcal{B}^{(o)}$  is neither block-diagonal nor block-off-diagonal.

Next the matrix  $Q(x, t)$  in (12) is taken to be block-off-diagonal, whose entries are assumed to be functions of  $x, t$  only. Its required property is just differentiability up to sufficiently high order while no relation among its entries is assumed.

The matrix  $T$ , see (12), satisfies the compatibility condition (3), which entails the following expression of the coefficients

$$\begin{aligned} T_2 &= C_2, \\ T_1 &= C_1 + I_1 + D_2(Q), \\ T_0 &= C_0 + I_0 + \frac{1}{2}[D_2(Q), \Gamma(Q)]^{(d)} + \\ &\quad + \Gamma(D_2(Q_x)) + \Gamma([D_2(Q), Q]^{(o)}) + D_1(Q) + [I_1, \Gamma(Q)], \end{aligned} \quad (16)$$

with the following comments and definitions. The matrices  $C_j$ ,  $j = 0, 1, 2$ , are constant and block-diagonal,  $C_j^{(o)} = 0$ . In the following we set  $C_0 = 0$ , because this matrix is irrelevant to our purposes. The notation  $\Gamma(\cdot)$  stands for the linear invertible map acting only on the subspace of the block-off-diagonal matrices (15b) according to the following definition and properties

$$(\Gamma(\mathcal{M}))_{jk} = \frac{\mathcal{M}_{jk}}{\alpha_j - \alpha_k}, \quad [\Sigma, \Gamma(\mathcal{M})] = \Gamma([\Sigma, \mathcal{M}]) = \mathcal{M}, \quad \mathcal{M}^{(d)} = 0, \quad (17)$$

which show that also the matrix  $\Gamma(\mathcal{M})$  is block-off-diagonal. Also the maps  $D_j(\cdot)$ ,  $j = 1, 2$ , act only on block-off-diagonal matrices according to the definitions

$$D_j(\mathcal{M}) = [C_j, \Gamma(\mathcal{M})], \quad \mathcal{M}^{(d)} = 0, \quad j = 1, 2. \quad (18)$$

Finally, the matrices  $I_j$ ,  $j = 1, 0$ , are block-diagonal and take the integral expression

$$I_1(x, t) = \int^x dy [Q(y, t), D_2(Q(y, t))]^{(d)}, \quad (19a)$$

$$\begin{aligned} I_0(x, t) &= \int^x dy \left\{ \frac{1}{2} [C_2, [\Gamma(Q_y(y, t)), \Gamma(Q(y, t))]^{(d)}] + \right. \\ &\quad + [Q(y, t), \Gamma([D_2(Q(y, t)), Q(y, t)]^{(o)})]^{(d)} + \\ &\quad \left. + [Q(y, t), D_1(Q(y, t))]^{(d)} + [Q(y, t), [I_1(t), \Gamma(Q(y, t))]^{(d)}] \right\}. \end{aligned} \quad (19b)$$

Because of (19), the matrix  $Q(x, t)$  evidently satisfies an integro-differential, rather than a partial differential, equation as a consequence of the compatibility condition (3). Incidentally, we note that this kind of non-locality generated by the Lax pair (2) has been already pointed out [13], while its solvability via spectral methods remains an open question. Here, however, we focus our attention on local equations only. Therefore the condition that  $Q(x, t)$  evolves according to a partial differential equation is equivalent to the vanishing of the matrices  $I_j$ ,  $j = 1, 0$ , which ultimately implies restrictions on the constant matrices  $C_1$  and  $C_2$ , as specified by the following

**Proposition 3** *The matrices  $I_1$  and  $I_0$  identically vanish if, and only if, the blocks of  $C_1$  and  $C_2$  are proportional to the identity matrix, namely*

$$C_1 = \text{diag}\{\beta_1 \mathbf{1}_1, \dots, \beta_L \mathbf{1}_L\}, \quad C_2 = \text{diag}\{\gamma_1 \mathbf{1}_1, \dots, \gamma_L \mathbf{1}_L\}. \quad (20)$$

Through the rest of the paper, we maintain these locality conditions so that the resulting evolution equation for the matrix  $Q$  reads

$$\begin{aligned} Q_t = & \Gamma(D_2(Q_{xx})) + [\Gamma(D_2(Q_x)), Q]^{(o)} + \Gamma([D_2(Q)], Q_x^{(o)}) + [(D_2(Q)\Gamma(Q))^{(d)}, Q] \\ & + [\Gamma([D_2(Q), Q]^{(o)}), Q]^{(o)} + D_1(Q_x) + [D_1(Q), Q]^{(o)}. \end{aligned} \quad (21)$$

This equation can be linearized around a given solution  $Q(x, t)$  by substituting  $Q$  with  $Q + \delta Q$  and by neglecting all nonlinear terms in the variable  $\delta Q$ . In this way we obtain the following linear PDE

$$\begin{aligned} \delta Q_t = & \Gamma(D_2(\delta Q_{xx})) + [\Gamma(D_2(\delta Q_x)), Q]^{(o)} + \Gamma([D_2(\delta Q_x), Q]^{(o)}) + \\ & + \Gamma([D_2(Q), \delta Q_x]^{(o)}) + [\Gamma(D_2(Q_x)), \delta Q]^{(o)} + \Gamma([D_2(Q_x), \delta Q]^{(o)}) + \\ & + \Gamma([D_2(\delta Q), Q_x]^{(o)}) + [(D_2(Q)\Gamma(Q))^{(d)}, \delta Q] + [(D_2(\delta Q)\Gamma(Q))^{(d)}, Q] + \\ & + [(D_2(Q)\Gamma(\delta Q))^{(d)}, Q] + [\Gamma([D_2(Q), Q]^{(o)}), \delta Q]^{(o)} + [\Gamma([D_2(\delta Q), Q]^{(o)}), Q]^{(o)} + \\ & + [\Gamma([D_2(Q), \delta Q]^{(o)}), Q]^{(o)} + D_1(\delta Q_x) + [D_1(Q), \delta Q]^{(o)} + [D_1(\delta Q), Q]^{(o)}. \end{aligned} \quad (22)$$

We are now in the position to formulate our next proposition which is the main result of this section.

**Proposition 4** *The matrix*

$$F = [\Sigma, \Phi], \quad (23)$$

*defined by (10), together with (12), satisfies the same linear PDE (22) satisfied by  $\delta Q$  if and only if the block-diagonal matrices  $C_1$  and  $C_2$  satisfy the same conditions (20) which guarantee the local character of the evolution equation (21).*

The proof of this result is obtained by straight computation, which is rather long and tedious, and is not reported here. We point out here just few hints on how to get it. The guiding idea is to eliminate the variable  $\lambda$  while combining the two ODEs (7) so as to obtain a PDE with  $\lambda$ -independent coefficients for the matrix  $F = [\Sigma, \Phi]$ . To this purpose, one starts by rewriting the first of the ODEs (7) for the block-diagonal  $\Phi^{(d)}$  and block-off-diagonal  $\Phi^{(o)} = \Gamma(F)$  components of  $\Phi$ , namely

$$\lambda F = \Gamma(F_x) - [Q, \Phi^{(d)}] - [Q, \Gamma(F)]^{(o)}, \quad \Phi_x^{(d)} = [Q, \Gamma(F)]^{(d)}. \quad (24)$$

Next, one considers the block-off-diagonal part of the second ODE of the pair (7) and replace  $\lambda F$  with its expression (24). The outcome of this substitution is that all terms containing the matrix  $\Phi^{(d)}$  do indeed cancel out, provided the conditions (20) are satisfied. The remaining terms of the expression of  $F_t$  can be rearranged as to coincide with those which appear in the PDE (22) by making use of algebraic matrix identities.

Few remarks are in order to illustrate these findings. The matrix

$$F = [\Sigma, \Psi M \Psi^{-1}]$$

(see (23) and (6)), which has the same block-off-diagonal structure (15b) of the matrix  $\delta Q$ , turns out to be a  $\lambda$ -dependent solution of the linearized equation (22). Its  $\lambda$ -dependence originates possibly from the (still arbitrary) matrix  $M$ , and certainly from the matrix solution  $\Psi$  of the Lax pair (2). Indeed,  $F$  plays the same role as the exponential solution of linear equations with constant coefficients, namely, by varying  $\lambda$  over a spectrum (see below), it provides the set of the ‘‘Fourier-like’’ modes of the linear PDE (22). This feature will be illustrated in the next section. In this respect we note that the property of the matrix  $F$  of satisfying the linearized PDE (22) does not depend on the boundary values of  $Q(x, t)$  at  $x = \pm\infty$ . In other words, this result applies as well to solutions  $Q(x, t)$  of the integrable PDE (21) with vanishing and non vanishing boundary values, or to periodic solutions, as required in various physical applications. Moreover, with appropriate reductions imposed on the matrix  $Q(x, t)$ , the integrable matrix PDE (21) associated to the Lax pair (2) with (12) includes, as special cases, wave propagation equations of physical relevance. Indeed, the PDE corresponding to  $L = 2$ ,  $N = 2$  and  $C_1 = 0$  yields the Nonlinear Schrödinger equation, while for its multicomponent versions (such as the vector or matrix generalizations of the NLS equation) one may set  $L = 2$ ,  $N > 2$  and  $C_1 = 0$ . By setting instead  $L = N > 2$  and  $C_2 = 0$ , one obtains the three wave resonant interaction system for  $N = 3$  [25], and many-wave interaction type equations for  $N > 3$  [4] (*e.g.*, see [11, 14, 15]).

## 2.1 $x$ -Spectrum $\mathbf{S}_x$ of the solution $Q(x, t)$

The result stated by Proposition 4 in the previous section implies that any sum and/or integral of  $F(x, t, \lambda)$  over the spectral variable  $\lambda$  is a solution  $\delta Q$  of the linear equation (22). Here and in the following, we assume that such linear combination of matrices  $F(x, t, \lambda)$ , which formally looks as the Fourier-like integral representation

$$\delta Q(x, t) = \int d\lambda F(x, t, \lambda) \quad (25)$$

is such to yield a solution  $\delta Q$  of (22) which is both *bounded* and *localized* in the  $x$  variable at any fixed time  $t$  (periodic perturbations  $\delta Q(x, t)$  are not considered here). The boundedness of  $\delta Q$  implies that the matrix  $F(x, t, \lambda)$  be itself bounded on the entire  $x$ -axis for any fixed value of  $t$  and for any of the values of  $\lambda$  which appear in the integral (25). This boundedness condition of  $F(x, t, \lambda)$  defines a special subset of the complex  $\lambda$ -plane, over which the integration runs, which will be referred to as the  $x$ -*spectrum*  $\mathbf{S}_x$  of the solution  $Q(x, t)$ . It obviously depends on the behaviour of the matrix  $Q(x)$  for large  $|x|$ . As shown below, this spectrum for  $N > 2$  *does not* coincide generically with the usual spectrum of the differential operator  $d/dx - i\lambda\Sigma - Q(x)$  defined by the ODE  $\Psi_x = X\Psi$  (say the  $x$ -part of the Lax pair (2)). It consists of a piecewise continuous curve and possibly of a finite number of isolated points. Note that at any point  $\lambda$  of the spectrum  $\mathbf{S}_x$  the matrices  $F(x, t, \lambda)$ , for any fixed  $t$ , span a functional space of matrices whose dimension depends on  $\lambda$ . Here we do not take up the issue of the completeness and closure of the set of matrices  $F(x, t, \lambda)$  and we rather consider solutions of (22) which have the integral representation

(25) and vanish sufficiently fast as  $|x| \rightarrow \infty$ , this being a requirement on the matrix  $M(\lambda)$  which appears in the definition (23) with (6). As in the standard linear stability analysis, the given solution  $Q(x, t)$  is then linearly stable if any initially small change  $\delta Q(x, t_0)$  remains small as time grows, say  $t > t_0$ . Thus, the basic ingredient of our stability analysis is the time-dependence of the matrices  $F(x, t, \lambda)$  for any  $\lambda \in \mathbf{S}_x$ . As we show below, getting this information requires knowing the spectrum  $\mathbf{S}_x$  whose computation therefore is our main goal.

### 3 Wave coupling and spectra: an example

In order to illustrate the results of the previous section and to capture, at the same time, a wide class of nonlinear wave phenomena of physical relevance (including the system of two coupled NLS equations), the rest of the paper will focus on the matrix case  $N = 3$ ,  $L = 2$ , with

$$\Sigma = \text{diag}\{1, -1, -1\} \quad (26)$$

and

$$Q = \begin{pmatrix} 0 & v_1^* & v_2^* \\ u_1 & 0 & 0 \\ u_2 & 0 & 0 \end{pmatrix}. \quad (27)$$

Here and below the asterisk denotes complex conjugation and the four field variables  $u_1, u_2, v_1, v_2$  are considered as independent functions of  $x$  and  $t$ , and are conveniently arranged as two two-dimensional vectors, that is

$$\mathbf{u} = \begin{pmatrix} u_1 \\ u_2 \end{pmatrix}, \quad \mathbf{v} = \begin{pmatrix} v_1 \\ v_2 \end{pmatrix}. \quad (28)$$

While we conveniently stick to this notation in this section, these formulae will be eventually reduced to those which lead to two coupled NLS equations as discussed in Section 3.3. Indeed, we note that adopting the non-reduced formalism (27), as we do it here, makes this presentation somehow simpler. In the present case all matrices are  $3 \times 3$  and the  $T$ -matrix (16) specializes to the expression

$$T(\lambda) = 2i\lambda^2\Sigma + 2\lambda Q + i\Sigma(Q^2 - Q_x), \quad (29)$$

while the matrix PDE (21) becomes

$$Q_t = -i\Sigma(Q_{xx} - 2Q^3), \quad (30)$$

which is equivalent to the two vector PDEs

$$\begin{aligned} \mathbf{u}_t &= i[\mathbf{u}_{xx} - 2(\mathbf{v}^\dagger \mathbf{u})\mathbf{u}] \\ \mathbf{v}_t &= i[\mathbf{v}_{xx} - 2(\mathbf{u}^\dagger \mathbf{v})\mathbf{v}]. \end{aligned} \quad (31)$$

Here the dagger notation denotes the Hermitian conjugation (which takes column-vectors into row-vectors). In this simpler setting, if  $Q(x, t)$  is a given solution of the equation (30), the linearized equation (22) for a small change  $\delta Q(x, t)$  reads

$$\delta Q_t = -i\Sigma[\delta Q_{xx} - 2(\delta Q Q^2 + Q \delta Q Q + Q^2 \delta Q)]. \quad (32)$$

Moreover, Proposition 4 guarantees that the matrix  $F(x, t, \lambda)$  satisfies this same linear PDE, namely

$$F_t = -i\Sigma[F_{xx} - 2(FQ^2 + QFQ + Q^2F)]. \quad (33)$$

and, for  $\lambda \in \mathbf{S}_x$ , these solutions should be considered as eigenmodes of the linearized equation.

The spectral analysis based on Proposition 4 applies to a large class of solutions  $Q(x, t)$  of the nonlinear wave equation (30). However, analytic computations are doable if the fundamental matrix solution  $\Psi(x, t, \lambda)$  of the Lax pair corresponding to the solution  $Q(x, t)$  is explicitly known. Examples are the vanishing and multisoliton (reflectionless) solutions. Here we devote our attention to the stability of the periodic continuous wave (CW) solution of (30), or of the equivalent vector system (31),

$$\mathbf{u}(x, t) = e^{i(qx\sigma_3 - \nu t)} \mathbf{a}, \quad \mathbf{v}(x, t) = e^{i(qx\sigma_3 - \nu t)} \mathbf{b}, \quad \nu = q^2 + 2\mathbf{b}^\dagger \mathbf{a}. \quad (34)$$

In these expressions  $a$  and  $b$  are arbitrary, constant and, with no loss of generality, real 2-dim vectors:

$$\mathbf{a} = \begin{pmatrix} a_1 \\ a_2 \end{pmatrix}, \quad \mathbf{b} = \begin{pmatrix} b_1 \\ b_2 \end{pmatrix}. \quad (35)$$

The interest in the system (31), or rather in its reduced version (see also Section 3.3), is motivated by both its wide applicability and by the fact that its NLS one-component version, for  $u_2 = v_2 = 0, v_1 = -u_1$ , turns out to be a good model of the Benjamin-Feir (or modulational) instability which is of great physical relevance [7, 22]. This kind of instability of the plane wave solution of the NLS equation occurs only in the self-focusing regime. In contrast, in the coupled NLS equations the cross interaction and the counterpropagation ( $q \neq 0$ ) introduce additional features (*e.g.*, see [21, 6]) which have no analogs in the NLS equation. This is so if the instability occurs even when the self-interaction terms have defocusing effects (see Section 3.3). Moreover, and by comparing the coupled case with the single field as in the NLS equation, we observe that this CW solution (34) depends on the real amplitudes  $a_1, a_2, b_1, b_2$ , and, in a crucial manner (see below), on the real parameter  $q$  which measures the *wave-number mismatch* between the two wave components  $u_1$  and  $u_2$  (or  $v_1$  and  $v_2$ ).

The main focus of this section is understanding how the spectrum  $\mathbf{S}_x$  changes by varying the parameters  $a_1, a_2, b_1, b_2$  and  $q$ . The results we obtain here will be specialized to the CNLS system in Section 3.3. In matrix notation, see (27), this continuous wave solution (34) reads

$$Q = R \Xi R^{-1}, \quad \Xi = \begin{pmatrix} 0 & b_1 & b_2 \\ a_1 & 0 & 0 \\ a_2 & 0 & 0 \end{pmatrix}, \quad R(x, t) = e^{i(qx\sigma - q^2 t \sigma^2 + pt \Sigma)}, \quad (36)$$

where the matrix  $\Sigma$  has the expression (26) while the matrix  $\sigma$  is

$$\sigma = \text{diag}\{0, 1, -1\} \quad (37)$$

and we conveniently introduce the real parameters

$$p = b_1 a_1 + b_2 a_2 \quad (38a)$$

$$r = b_1 a_1 - b_2 a_2 \quad (38b)$$

which will be handy in the following. Next we observe that a fundamental matrix solution  $\Psi(x, t, \lambda)$  of the Lax equations has the expression

$$\Psi(x, t, \lambda) = R(x, t) e^{i(xW(\lambda) - tZ(\lambda))}, \quad (39)$$

where the  $x, t$ -independent matrices  $W$  and  $Z$  are found to be

$$W(\lambda) = \begin{pmatrix} \lambda & -ib_1 & -ib_2 \\ -ia_1 & -\lambda - q & 0 \\ -ia_2 & 0 & -\lambda + q \end{pmatrix} = \lambda \Sigma - q\sigma - i\Xi, \quad (40)$$

$$Z(\lambda) = \begin{pmatrix} -2\lambda^2 & i(2\lambda - q)b_1 & i(2\lambda + q)b_2 \\ i(2\lambda - q)a_1 & 2\lambda^2 - q^2 - a_2 b_2 & a_1 b_2 \\ i(2\lambda + q)a_2 & a_2 b_1 & 2\lambda^2 - q^2 - a_1 b_1 \end{pmatrix} = \lambda^2 - 2\lambda W(\lambda) - W^2(\lambda) - p^2, \quad (41)$$

with the property that they commute,  $[W, Z] = 0$ , consistently with the compatibility condition (3). In order to proceed with plain arguments, we consider here the eigenvalues  $w_j(\lambda)$  and  $z_j(\lambda)$ ,  $j = 1, 2, 3$ , of  $W(\lambda)$  and, respectively, of  $Z(\lambda)$  as simple, as indeed they are for generic values of  $\lambda$ . In this case both  $W(\lambda)$  and  $Z(\lambda)$  are diagonalized by the same matrix  $U(\lambda)$ , namely

$$\begin{aligned} W(\lambda) &= U(\lambda) W_D(\lambda) U^{-1}(\lambda), & W_D &= \text{diag}\{w_1, w_2, w_3\} \\ Z(\lambda) &= U(\lambda) Z_D(\lambda) U^{-1}(\lambda), & Z_D &= \text{diag}\{z_1, z_2, z_3\}. \end{aligned} \quad (42)$$

Next we construct the matrix  $F(x, t, \lambda)$  via its definition, see (23) and (6),

$$F(x, t, \lambda) = [\Sigma, \Psi(x, t, \lambda) M(\lambda) \Psi^{-1}(x, t, \lambda)], \quad (43)$$

which, because of the explicit expression (39), reads

$$F(x, t, \lambda) = R(x, t) \left[ \Sigma, e^{i(xW(\lambda) - tZ(\lambda))} M(\lambda) e^{-i(xW(\lambda) - tZ(\lambda))} \right] R^{-1}(x, t). \quad (44)$$

As for the matrix  $M(\lambda)$ , it lies in a nine-dimensional linear space whose standard basis is given by the matrices  $B^{(jm)}$ , whose entries are

$$B_{kn}^{(jm)} = \delta_{jk} \delta_{mn}, \quad (45)$$

where  $\delta_{jk}$  is the Kronecker symbol ( $\delta_{jk} = 1$  if  $j = k$  and  $\delta_{jk} = 0$  otherwise). However the alternative basis  $V^{(jm)}$ , which is obtained via the similarity transformation

$$V^{(jm)}(\lambda) = U(\lambda) B^{(jm)} U^{-1}(\lambda), \quad (46)$$

where  $U(\lambda)$  diagonalizes  $W$  and  $Z$  (see (42)), is more convenient to our purpose. Indeed, expanding the generic matrix  $M(\lambda)$  in this basis as

$$M(\lambda) = \sum_{j,m=1}^3 \mu_{jm}(\lambda) V^{(jm)}(\lambda), \quad (47)$$

the scalar functions  $\mu_{jm}$  being its components, and inserting this decomposition into the expression (44), leads to the following representation of  $F$

$$F(x, t, \lambda) = R(x, t) \sum_{j,m=1}^3 \mu_{jm}(\lambda) e^{i[(x(w_j-w_m)-t(z_j-z_m))]} F^{(jm)}(\lambda) R^{-1}(x, t), \quad (48)$$

where we have introduced the  $x, t$ -independent matrices

$$F^{(jm)}(\lambda) = \left[ \Sigma, V^{(jm)}(\lambda) \right]. \quad (49)$$

The advantage of expression (48) is to explicitly show the dependence of the matrix  $F$  on the six exponentials  $e^{i[(x(w_j-w_m)-t(z_j-z_m))]}$ .

The Proposition 4 stated in the previous section guarantees that, for any choice of the functions  $\mu_{jm}(\lambda)$ , the expression (48) be a solution of the linearized equation (32), see (33). It is plain (see (25)) that the requirement that such solution  $\delta Q(x, t)$  be localized in the variable  $x$  implies the necessary condition that the functions  $\mu_{jm}(\lambda)$  be vanishing for  $j = m$ ,  $\mu_{jj} = 0$ ,  $j = 1, 2, 3$ . The further condition that the solution  $\delta Q(x, t)$  be bounded in  $x$  at any fixed time  $t$  results in integrating expression (48) with respect to the variable  $\lambda$  over the spectral curve  $\mathbf{S}_x$  of the complex  $\lambda$ -plane (see (25)):

$$\delta Q(x, t) = \int_{\mathbf{S}_x} d\lambda F(x, t, \lambda). \quad (50)$$

Here, according to Section 2.1,  $\mathbf{S}_x$  can be geometrically defined as follows:

**Definition 1** *The  $x$ -spectrum  $\mathbf{S}_x$ , namely the spectral curve on the complex  $\lambda$ -plane, is the set of values of the spectral variable  $\lambda$  such that at least one of the three complex numbers  $k_j = w_{j+1} - w_{j+2}$ ,  $j = 1, 2, 3 \pmod{3}$ , or explicitly*

$$k_1(\lambda) = w_2(\lambda) - w_3(\lambda), \quad k_2(\lambda) = w_3(\lambda) - w_1(\lambda), \quad k_3(\lambda) = w_1(\lambda) - w_2(\lambda), \quad (51)$$

is real.

Observe that the  $k_j$ 's play the role of eigenmode wave-numbers (see (48)).

To the purpose of establishing the stability properties of the continuous wave solution (34) we do not need to compute the integral representation (50) of the solution  $\delta Q$  of (32). Indeed, it is sufficient to compute the eigenfrequencies

$$\omega_1(\lambda) = z_2(\lambda) - z_3(\lambda), \quad \omega_2(\lambda) = z_3(\lambda) - z_1(\lambda), \quad \omega_3(\lambda) = z_1(\lambda) - z_2(\lambda), \quad (52)$$

as suggested by the exponentials which appear in (48). Their expression follows from the matrix relation (41)

$$z_j = \lambda^2 - 2\lambda w_j - w_j^2 - p, \quad (53)$$

and read

$$\omega_j = -k_j(2\lambda + w_{j+1} + w_{j+2}), \quad j = 1, 2, 3 \pmod{3}. \quad (54)$$

This expression looks even simpler by using the relation  $w_1 + w_2 + w_3 = -\lambda$  implied by the trace of the matrix  $W(\lambda)$  (see (40)) and finally reads

$$\omega_j = k_j(w_j - \lambda), j = 1, 2, 3. \quad (55)$$

The consequence of this expression (55), which is relevant to our stability analysis, is given by the following

**Proposition 5** *The continuous wave solution (34) is stable against perturbations  $\delta Q$  whose representation (25) is given by an integral which runs only over those values of  $\lambda \in \mathbf{S}_x$  which are strictly real.*

**Proof** The reality of the spectral variable  $\lambda$  implies that all coefficients of the characteristic polynomial of the matrix  $W(\lambda)$  (40),

$$P_W(w; \lambda) = \det[w\mathbf{1} - W(\lambda)] = w^3 + \lambda w^2 + (p - q^2 - \lambda^2)w - \lambda^3 + (p + q^2)\lambda - qr, \quad (56)$$

are real. Indeed, these coefficients depend on the real parameters of the CW solution (34), namely the wavenumber mismatch  $q$ , the parameters  $p$  and  $r$  defined by (38). Its roots  $w_j$  are therefore either all real or one real and two complex conjugate. In the first case the three wave-numbers  $k_j$  (51) are all real and therefore the corresponding  $\lambda$  is in the spectrum  $\mathbf{S}_x$ ,  $\lambda \in \mathbf{S}_x$ . In the second case the three  $k_j$  are all complex, *i.e.* with non vanishing imaginary part, and therefore  $\lambda$  lies in a forbidden interval of the real axis which does not belong to the spectrum  $\mathbf{S}_x$ ,  $\lambda \notin \mathbf{S}_x$ . In the following we refer to one such forbidden real interval as a *gap*, see the Subsection 3.1 below. Thus, in the first case, since  $\lambda$ ,  $w_1$ ,  $w_2$ ,  $w_3$  and therefore,  $k_1$ ,  $k_2$ ,  $k_3$ , are all real, then also  $\omega_1$ ,  $\omega_2$ ,  $\omega_3$ , see (55), are all real, with the implication of stability. Indeed, all eigenmode matrices (48) remain small at all times if they are so at the initial time. Finally, it should be pointed out that Proposition 5 remains valid for any value of the parameters  $q$ ,  $p$  and  $r$ .  $\square$

This Proposition 5 implies that a real part of the spectrum  $\mathbf{S}_x$  is always present, and this part may or may not have gaps (see the next Subsection 3.1). On the contrary, as it will be proved below (see Subsection 3.2), a complex component of the spectrum, namely one which lies off the real axis of the  $\lambda$ -plane, may occur and it always leads to instabilities. This important part of the spectrum  $\mathbf{S}_x$  is made of open curves, which will be referred to as *branches*, and/or closed curves of the complex  $\lambda$ -plane which will be termed *loops*.

Before proceeding further we observe that the effect of the cross interaction is crucially influent on the stability only if the phases of the two continuous waves (34) have different  $x$ -dependence, namely if  $q \neq 0$  (see (34)). Indeed, if  $q = 0$  the stability property of the continuous wave is essentially that of the NLS equation. This conclusion results from the explicit formulae  $w_1 = \sqrt{\lambda^2 - p}$ ,  $w_2 = -\sqrt{\lambda^2 - p}$ ,  $w_3 = -\lambda$ , and therefore

$$\begin{aligned} k_1 &= \lambda - \sqrt{\lambda^2 - p}, & k_2 &= -\lambda - \sqrt{\lambda^2 - p}, & k_3 &= 2\sqrt{\lambda^2 - p}, \\ \omega_1 &= -2\lambda^2 + p + 2\lambda\sqrt{\lambda^2 - p}, & \omega_2 &= 2\lambda^2 - p + 2\lambda\sqrt{\lambda^2 - p}, & \omega_3 &= -4\lambda\sqrt{\lambda^2 - p}, \end{aligned} \quad (57)$$

which show that if  $p > 0$  (see (38a)) the spectrum  $\mathbf{S}_x$  is the real axis with the exclusion of the gap  $\{-\sqrt{p} < \lambda < \sqrt{p}\}$ , while, if  $p < 0$ , the spectrum  $\mathbf{S}_x$  is the entire real axis with the

addition of the imaginary branch  $\lambda = i\rho$ ,  $\{-\sqrt{-p} < \rho < \sqrt{-p}\}$ . Therefore, the stability for  $p > 0$  follows from the reality of the frequencies  $\omega_1, \omega_2, \omega_3$  over the whole spectrum  $\mathbf{S}_x$ , see (57). The modulational instability occurs only if  $p < 0$  since, for  $\lambda$  in the imaginary branch of the spectrum  $\mathbf{S}_x$ , the frequencies  $\omega_1, \omega_2$  and  $\omega_3$  have a non vanishing imaginary part.

In the following, while computing the spectrum  $\mathbf{S}_x$ , we consider therefore only the case  $q \neq 0$  and, with no loss of generality, strictly positive,  $q > 0$ . In this respect, we also note that the assumption that  $q$  be non-vanishing makes it possible, without any loss of generality, to rescale it to unit,  $q = 1$ , while keeping in mind that, by doing so,  $\lambda, w_j$  rescale as  $q$  while  $p, r, z_j$  rescale as  $q^2$ , *i.e.*

$$\lambda \mapsto q\lambda, \quad w \mapsto qw, \quad p \mapsto q^2p, \quad r \mapsto q^2r, \quad z \mapsto q^2z.$$

However, we deem it helpful to the reader to maintain the parameter  $q$  in our formulae, here and in the following, to have a good control of the limit as  $q$  vanishes. In addition, here and thereafter, our computations and results will be formulated for non-negative values of the parameter  $r$  according to the following

**Proposition 6** *With no loss of generality, the relevant parameter space reduces to the half  $(r, p)$ -plane with  $r \geq 0$ .*

Indeed, the change of sign  $\lambda \mapsto -\lambda, r \mapsto -r$  takes the characteristic polynomial  $P_W(w; \lambda)$  (56) into  $-P_W(-w; \lambda)$  and this implies that our attention may be confined to non-negative values of  $r$  only.

### 3.1 Gaps

Although computing the position of the gaps of  $\mathbf{S}_x$  on the real  $\lambda$ -axis is not strictly relevant to the issue of stability because of Proposition 5, this information is essential to the construction of soliton solutions corresponding to real discrete eigenvalues which lie inside a gap. With this motivation in mind, we devote this subsection to this task. Using the Cardano formulae for finding workable explicit expressions of the three roots  $w_j(\lambda)$  of  $P_W(w; \lambda)$  for each value of  $p, r$  and  $q$  is not practical. To overcome this difficulty, we will adopt here an algebraic-geometric approach.

We begin by computing the discriminant  $D_W = \Delta_w P_W(w; \lambda)$  of the polynomial  $P_W(w; \lambda)$  (56) with respect to  $w$ , obtaining thus a polynomial in  $\lambda$ , with parameters  $q, p, r$ ,

$$D_W(\lambda; q, p, r) = 64q^2\lambda^4 - 32qr\lambda^3 + 4(p^2 - 20q^2p - 8q^4)\lambda^2 + 36qr(2q^2 + p)\lambda - 4(p - q^2)^3 - 27q^2r^2, \quad (58)$$

which is *positive* whenever the three roots  $w_j$  are real, and it is *negative* if instead only one root is real. Consequently, for any given value of the parameters  $q, p$ , and  $r$ , the discriminant is negative,  $D_W < 0$ , for those real values of  $\lambda$  which belong to a gap of  $\mathbf{S}_x$ , while its zeros are the end points of gaps. Here and hereafter the notation  $\Delta_y P(x, y, z)$  stands for the discriminant of the polynomial  $P$  with respect to its variable  $y$ .

In the exceptional case  $r = 0$ , computing the roots of the discriminant  $D_W$  as a polynomial in the variable  $\lambda$  reduces to the factorization of a quadratic polynomial, allowing the formulation of the following

**Proposition 7** *For  $r = 0$ , the gaps depend on the parameter  $p$  as follows:*

$-\infty < p < 0$	<i>no gap</i>
$0 \leq p < q^2$	<i>two gaps, <math>-g_+ \leq \lambda \leq -g_-</math> and <math>g_- \leq \lambda \leq g_+</math></i>
$q^2 \leq p < +\infty$	<i>one gap, <math>-g_+ \leq \lambda \leq g_+</math></i>

The border values  $g_{\pm}$  are

$$g_{\pm} = \frac{\sqrt{2}}{8q} \sqrt{8q^4 + 20q^2p - p^2 \pm \sqrt{p(p + 8q^2)^3}}. \quad (59)$$

The threshold values  $p = 0$  and  $p = q^2$  correspond to the opening and the coalescence of two gaps, respectively.

In the generic case  $r \geq 0$  we find that the number of gaps of the real part of the spectrum  $\mathbf{S}_x$  is either zero, or one, or two. Gaps appear at double-zeros of the discriminant  $D_W(\lambda; q, p, r)$ , thus at zeros of its own discriminant  $\Delta_{\lambda} D_W(\lambda; q, p, r) = \Delta_{\lambda} \Delta_w P_W(w; \lambda)$ , namely when

$$\Delta_{\lambda} D_W(\lambda; q, p, r) = -1048576 (p - r) (p + r) [(p - 1) (p + 8)^2 - 27 r^2]^3 = 0. \quad (60)$$

The three polynomial factors appearing in (60) bound the regions of the  $(r, p)$ -plane characterized by different numbers of gaps.

By varying the values of the parameters  $q$ ,  $p$ , and  $r$ , we expect the double-zeros to open and form the gaps, namely intervals where  $D_W < 0$ . In order to find the number of gaps from the expression (58) of the discriminant  $D_W(\lambda; q, p, r)$ , it is convenient to plot the dependence of the parameter  $p = p(\lambda)$  on the spectral variable  $\lambda$  at the zeros of this discriminant for fixed values of the parameters  $r$  and  $q$ . This function  $p(\lambda)$  is therefore implicitly defined by the equation  $D_W(\lambda; q, p(\lambda), r) = 0$ . For a fix value of  $q$ , which without loss of generality we choose to be 1, in the  $(\lambda, p)$ -plane the  $p(\lambda)$  curve has always one cusp (a double singular point), and either two minima, or one minimum and one maximum, depending on the value of  $r$  (see Appendix A for details). The position of the cusp  $(\lambda_S, p_S)$  as a function of  $r$  and  $q$  is

$$\lambda_S(r) = \frac{3}{2} \left\{ \left[ (qr/2) + \sqrt{q^6 + (qr/2)^2} \right]^{1/3} - q^2 \left[ (qr/2) + \sqrt{q^6 + (qr/2)^2} \right]^{-1/3} \right\}, \quad (61)$$

$$p_S(r) = q^2 + \frac{4}{3} \lambda_S^2(r).$$

Furthermore,  $p_S(r)$  seen as an algebraic curve in the  $(r, p)$ -plane satisfies the following implicit relation

$$(p - q^2) (p + 8q^2)^2 - 27 r^2 q^2 = 0, \quad p = p_S(r). \quad (62)$$

The transition between the two regimes (two minima, or one minimum and one maximum) takes place at the special threshold value  $r_T = 4q^2$  where  $p_S(r_T) = r_T$  (see Appendix A). If  $0 \leq r < r_T$  the cusp is also a local maximum. Equipped with these findings, we formulate

**Proposition 8** For real  $\lambda$  and  $r > 0$ ,  $\mathbf{S}_x$  has the following gap structure.

If  $r < r_T = 4q^2$

$-\infty < p < -r$	no gap
$-r \leq p < r$	one gap
$r \leq p < p_S(r)$	two gaps
$p_S(r) \leq p < +\infty$	one gap

The threshold values  $p = -r$ ,  $p = r$ , and  $p = p_S(r)$  correspond to the opening of one gap, the opening of two gaps, and the coalescence of two gaps, respectively.

If  $r > r_T = 4q^2$

$-\infty < p < -r$	no gap
$-r \leq p < p_S(r)$	one gap
$p_S(r) \leq p < r$	two gaps
$r \leq p < +\infty$	one gap

The threshold values  $p = -r$ ,  $p = p_S(r)$ , and  $p = r$  correspond to the opening of one gap, the opening of two gaps, and the coalescence of two gaps, respectively.

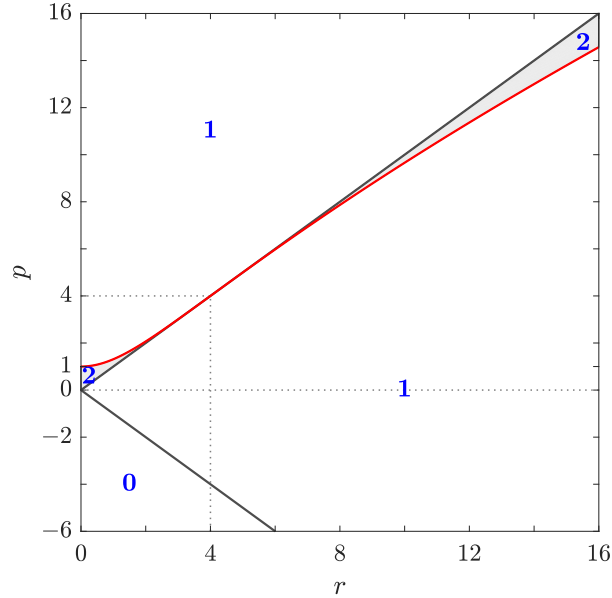


Figure 1: The three threshold curves  $p_{\pm}(r) = \pm r$  (solid black) and  $p_S(r)$  (solid red) for  $q = 1$ , as parametrically defined by (63) and (62) or explicitly by (61), are plotted. They are boundaries of regions of the  $(r, p)$ -plane,  $r > 0$ , where the number of gaps, either 0, or 1, or 2, is shown. It is also shown that  $p_S(r) > r$  for  $r < 4$ , and that  $p_S(r) < r$  for  $r > 4$  (see Proposition 8).

As implied by (60) and Proposition 8, we identify three threshold curves in the  $(r, p)$ -half-plane; they are

$$p = p_{\pm}(r) = \pm r \quad (63)$$

and the curve  $p = p_S(r)$  which is explicitly expressed by (61) and plotted in Figure 1. Note that, according to Proposition 6, we will focus only on the half-plane  $r \geq 0$ . These curves will play a role also in the next subsection where we give a complete classification of branches and loops of the spectrum.

### 3.2 Branches and loops

In the previous subsection we have described the gaps of the spectrum  $\mathbf{S}_x$ , namely those values of the spectral parameter  $\lambda$  which are real but do not belong to the spectrum. Here we face instead the problem of finding the subset of the  $\lambda$ -plane which is off the real axis but belongs to  $\mathbf{S}_x$ . This subset is generally made of finite and smooth, open (branches) or closed (loops), continuous curves. By Definition 1,  $\lambda \in \mathbf{S}_x$  if at least one of the corresponding three wave numbers  $k_j(\lambda)$ ,  $j = 1, 2, 3$  is real, see (51). Going back to the characteristic polynomial  $P_W(w; \lambda)$  (56), we look now at its roots  $w_j$ , and at the wave numbers  $k_j$ ,  $j = 1, 2, 3$ , see (51). If  $\lambda$  is not real, the roots  $w_j$  cannot be all real themselves since the coefficients of  $P_W(w; \lambda)$  are not real. As a consequence, the requirement that one of the wave numbers (51) be real implies that at least two roots of  $P_W(w; \lambda)$ , for instance  $w_1$  and  $w_2$ , have the same imaginary part. In fact, branches and loops of  $\mathbf{S}_x$  may exist only in this case: indeed, if the three roots  $w_j$  have all the same imaginary part, it can be shown that no smooth branch or loop exists. Hence, here and below, we name  $k_3 = w_1 - w_2$  the only real wave number, while  $k_1$  and  $k_2$  are complex (note that  $k_1 + k_2 + k_3 = 0$ ). The complex part of the spectrum  $\mathbf{S}_x$  is therefore defined as the set of the  $\lambda$ -plane such that  $\text{Im}(k_3(\lambda)) = 0$ . In order to compute this component of the spectrum, we introduce the novel polynomial  $\mathcal{P}(\zeta)$ ,

$$\mathcal{P}(\zeta) = \zeta^3 + d_1\zeta^2 + d_2\zeta + d_3, \quad (64)$$

defined by the requirement that its roots are the squares of the wave numbers,  $\zeta_j = k_j^2$ . It is plain that its coefficients  $d_j$  are completely symmetric functions of the roots  $w_j$  of the characteristic polynomial  $P_W(w; \lambda)$ . This is evidently so because  $d_1, d_2, d_3$  are symmetric functions of  $\zeta_1 = (w_2 - w_3)^2$ ,  $\zeta_2 = (w_3 - w_1)^2$ ,  $\zeta_3 = (w_1 - w_2)^2$ , and therefore of  $w_1, w_2, w_3$ , with the implication that the coefficients  $d_1, d_2, d_3$  of  $\mathcal{P}(\zeta)$  are polynomial functions of the coefficients  $c_1, c_2, c_3$  of the characteristic polynomial (56),  $P_W(w) = w^3 + c_1w^2 + c_2w + c_3$ ,

$$c_1 = \lambda, \quad c_2 = p - q^2 - \lambda^2, \quad c_3 = -\lambda^3 + (p + q^2)\lambda - qr. \quad (65)$$

These relations, which read

$$\begin{aligned} d_1 &= 2(3c_2 - c_1^2), \\ d_2 &= (3c_2 - c_1^2)^2 = \frac{1}{4}d_1^2, \\ d_3 &= (4c_2 - c_1^2)(c_2^2 - 4c_1c_3) + c_3(27c_3 - 2c_1c_2), \end{aligned} \quad (66)$$

combined with the expressions of the coefficients  $c_j$ , see (65), yield the dependence of the coefficients  $d_j$  of  $\mathcal{P}(\zeta)$  on the parameters  $r, p, q$  and on the spectral variable  $\lambda$ , so that  $\mathcal{P}(\zeta) \equiv \mathcal{P}(\zeta; \lambda, q, p, r)$ . This dependence turns out to be

$$d_1 = 2[-4\lambda^2 + 3(p - q^2)], \quad d_2 = [-4\lambda^2 + 3(p - q^2)]^2, \quad d_3 = -D_W(\lambda; q, p, r), \quad (67)$$

where  $D_W$  is the discriminant of  $P_W$ , see its expression (58). As explained at the beginning of this section, we recall that, for an arbitrary complex  $\lambda$ , at most one wave number (named  $k_3$ ) is real. Therefore our task of computing the complex part of the spectrum  $\mathbf{S}_x$ , for a given value of the parameters  $r, p$ , reduces to finding the curve in the  $\lambda$ -plane along which the root  $\zeta_3(\lambda) = k_3^2(\lambda)$  of  $\mathcal{P}(\zeta; \lambda, q, p, r)$  remains *real and positive*,  $\zeta_3 = k_3^2 > 0$ . However, it is in general much more convenient, from both the analytical and computational points of view, (and indeed this is what we will be doing in the following), to reverse the perspective and regard the  $x$ -spectrum  $\mathbf{S}_x$  as the *locus* in the  $\lambda$ -plane of the  $\lambda$ -roots of  $\mathcal{P}(\zeta; \lambda, q, p, r)$  seen as a *real* polynomial in  $\lambda$ , for  $\zeta$  spanning over the semi-line  $[0, +\infty)$ . In other words, for a fixed value of  $\zeta \geq 0$ , we compute the four  $\lambda$ -roots of the real polynomial  $\mathcal{P}(\zeta; \lambda, q, p, r)$ , which are the values of  $\lambda$  (irrespective of being complex or purely real) such that the wave number  $k_3 = \sqrt{\zeta}$  is real. In this way, the two cases of  $\text{Im}(\lambda) = 0$  and  $\text{Im}(\lambda) \neq 0$  can be treated at once (allowing to retrieve and confirm all the results about gaps in the spectra presented in the previous subsection).

From the algebraic-geometric point of view, the locus of the roots of  $\mathcal{P}(\zeta; \lambda, q, p, r)$  in the  $\lambda$ -plane is an algebraic curve; this can be given explicitly as a system of two polynomial equations in two unknowns by setting  $\lambda = \mu + i\rho$  and then separating the real and the imaginary parts of  $\mathcal{P}(\zeta; \lambda, q, p, r)$ .

In order to explain how the spectrum changes over the parameter space, we apply Sturm's chains (*e.g.*, see [18, 23]) to the polynomial  $\mathcal{Q}(\zeta; q, p, r) = \Delta_\lambda \mathcal{P}(\zeta; \lambda, q, p, r)$ , that is, to the discriminant of the polynomial  $\mathcal{P}(\zeta; \lambda, q, p, r)$  with respect to  $\lambda$ . Indeed, it turns out that the nature and the number of the components of the  $x$ -spectrum  $\mathbf{S}_x$ , seen as a curve in the  $\lambda$ -plane, are classified by the number of sign-changes of  $\mathcal{Q}(\zeta; q, p, r)$ , for  $\zeta \geq 0$ . This procedure requires some technical digression, thus, in order to avoid breaking the narrative here, we refer the reader to Appendix B for all details.

Our findings provide a complete classification of the spectra over the entire parameter space, *i.e.* over the  $(r, p)$ -plane,  $r \geq 0$ . First we note that the number of branches (B) can only be 0, 1, or 2, while there may occur either 0, or 1 loop (L). Moreover, in addition to the three threshold curves  $p_\pm(r)$  (63) and  $p_S(r)$  (61) introduced in Subsection 3.1, one more threshold curve,  $p = p_C(r)$ , is found, which, for a given non vanishing value of  $q$ , is implicitly defined as

$$(p^2 - 16q^4)^3 + 432q^4r^2(p^2 - r^2) = 0, \quad p = p_C(r), \quad \text{with } p < 0, \quad (68)$$

or, explicitly, as

$$p_C(r) = -\sqrt{16 - 12(2r)^{2/3} + 3(2r)^{4/3}}. \quad (69)$$

It is now convenient to combine these results with those we obtained in the previous subsection on the gaps (G) on the real  $\lambda$ -axis of the complex  $\lambda$ -plane, obtaining a complete classification of the spectra. We find that only five different types of spectra exist according to different combinations of gaps, branches and loops. These are the following:

$$0\text{G } 2\text{B } 0\text{L}, \quad 0\text{G } 2\text{B } 1\text{L}, \quad 1\text{G } 1\text{B } 0\text{L}, \quad 1\text{G } 1\text{B } 1\text{L}, \quad 2\text{G } 0\text{B } 1\text{L},$$

where the notation  $n\text{X}$  stands for  $n$  components of the type X, with X either G, or B, or L.

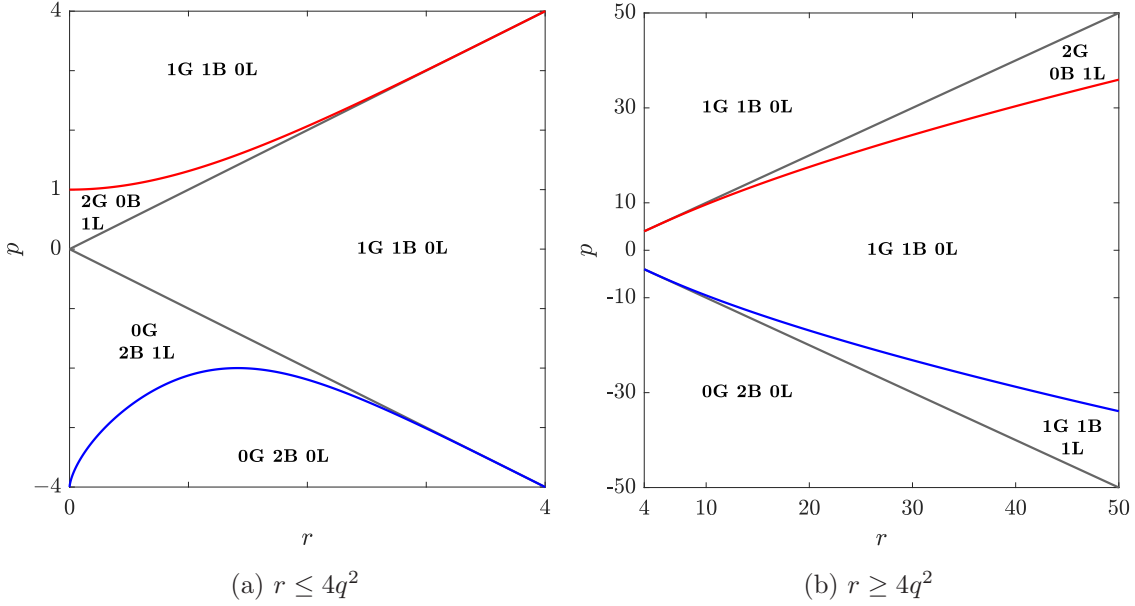


Figure 2: The structure of the spectrum  $\mathbf{S}_x$  in the  $(r, p)$  plane,  $q = 1$  (see Proposition 9).

In Figure 2 the four threshold curves  $p_{\pm}$ ,  $p_S$ ,  $p_C$  (with  $q = 1$ ) are plotted to show the partition of the parameter half-plane according to the gap, branch and loop components of the spectrum, both for  $r < r_T = 4q^2$ , and  $r > r_T = 4q^2$ . This overall structure of the spectrum  $\mathbf{S}_x$  in the parameter space can be summarized by the following

**Proposition 9** For  $r \geq 0$ , the spectrum  $\mathbf{S}_x$  has the following structure in the parameter plane  $(r, p)$ .

If  $r < r_T = 4q^2$

$-\infty < p < p_C(r)$	0G 2B 0L
$p_C(r) < p < -r$	0G 2B 1L
$-r < p < r$	1G 1B 0L
$r < p < p_S(r)$	2G 0B 1L
$p_S(r) < p < +\infty$	1G 1B 0L

If  $r > r_T = 4q^2$

$-\infty < p < -r$	0G 2B 0L
$-r < p < p_C(r)$	1G 1B 1L
$p_C(r) < p < p_S(r)$	1G 1B 0L
$p_S(r) < p < r$	2G 0B 1L
$r < p < +\infty$	1G 1B 0L

At the threshold values, gaps, branches and loops open up from, or coalesce into points, as can be inferred by comparing the structure before and after the threshold: for instance, for

$r < 4q^2$  and  $p = p_S(r)$ , one gap coalesces into a point, one branch opens up from a point, and a loop coalesces into a point.

Examples of different spectra have been computed numerically by calculating the zeros of  $\mathcal{P}(\zeta; \lambda, q, p, r)$  as a polynomial in  $\lambda$  (see Appendix C for details), and are displayed in Figure 3. They are representative of the five types, and correspond to various points of the parameter  $(r, p)$ -space as reported in Proposition 9.

Finally, the limit case  $r = 0$  of the parameter half-plane  $r > 0$  deserves a special mention. In fact, four different limit spectra are found for  $r = 0$ , namely in the four intervals  $-\infty < p < -4q^2$ ,  $-4q^2 < p < 0$ ,  $0 < p < q^2$  and  $q^2 < p < +\infty$ . After meticulous analysis (see [17]) we find that these limit spectra are consistent with those depicted by Proposition 9. However, they have to be carefully dealt with as, in this limit, two gaps may coalesce in one, or a loop may go through the point at infinity of the  $\lambda$ -plane thereby covering the whole imaginary axis. These spectra are displayed in Figures 3f, 3g and 3h. We should also point out that the condition  $r = 0$  allows for analytic computations, and explicit formulae, since, as already noted in Subsection 3.1 for the discriminant  $D_W(\lambda; q, p, r)$ , the coefficients  $d_j(\lambda)$  of the relevant polynomial  $\mathcal{P}(\zeta; \lambda, q, p, r)$  (64) reduce to polynomials of degree 2 in the variable  $\lambda^2$ .

### 3.3 Modulational instability of two coupled NLS equations

In this section we discuss the consequences of the results obtained so far in the framework of the study of the instabilities of a system of two coupled NLS equations.

In the scalar case, the focusing NLS equation

$$u_t = i(u_{xx} - 2s|u|^2u), \quad s = -1 \quad (70)$$

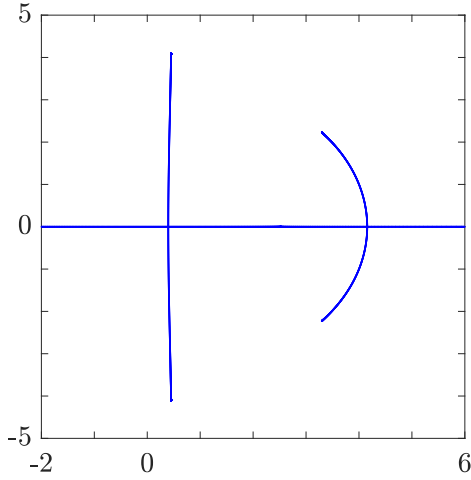
has played an important role in modelling modulational instability of continuous waves [7, 22]. This unstable behavior is predicted for this equation by simple arguments and calculations. It is therefore rather remarkable that, on the contrary, a nonlinear coupling of two NLS equations makes the unstable dynamics of two interacting continuous waves fairly richer than that of a single wave. Since the method of investigating the stability of two coupled NLS equations that we have presented in the previous sections requires integrability, we deal here with the integrable system (1), also known as *generalized Manakov model*, that we recall here for convenience:

$$\begin{aligned} u_{1t} &= i[u_{1xx} - 2(s_1|u_1|^2 + s_2|u_2|^2)u_1] \\ u_{2t} &= i[u_{2xx} - 2(s_1|u_1|^2 + s_2|u_2|^2)u_2]. \end{aligned}$$

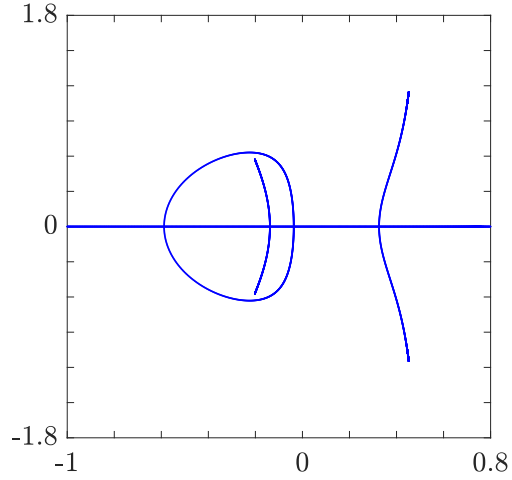
This system is obtained by setting  $\mathbf{v} = S\mathbf{u}$  in (31), where

$$S = \begin{pmatrix} s_1 & 0 \\ 0 & s_2 \end{pmatrix}, \quad S^2 = \mathbf{1}. \quad (71)$$

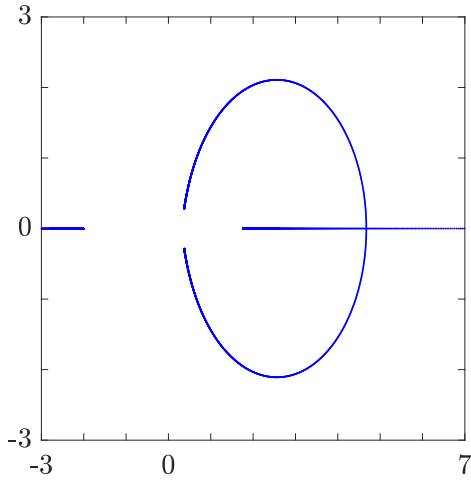
The system of two coupled NLS equations is of interest in various physical contexts and the investigation of the stability of its solutions deserves special attention.



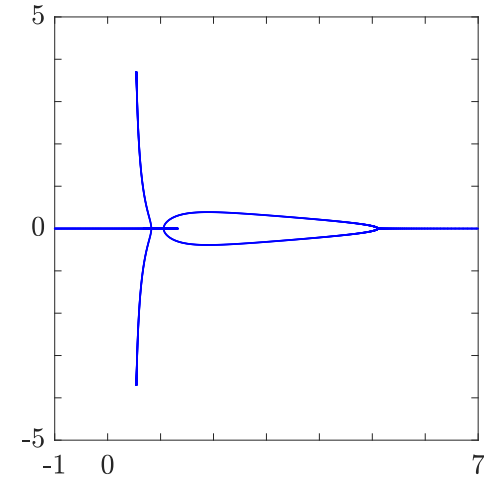
(a)  $\mathbf{S}_x$  for  $r = 15$ ,  $p = -17$ , *i.e.*,  $s_1 = s_2 = -1$ ,  $a_1 = 1$ ,  $a_2 = 4$ , as an example of a 0G 2B 0L spectrum.



(b)  $\mathbf{S}_x$  for  $r = 1$ ,  $p = -1.5$ , *i.e.*,  $s_1 = s_2 = -1$ ,  $a_1 = 0.5$ ,  $a_2 = 1.118$ , as an example of a 0G 2B 1L spectrum.



(c)  $\mathbf{S}_x$  for  $r = 1$ ,  $p = 2.8$ , *i.e.*,  $s_1 = s_2 = 1$ ,  $a_1 = 1.3784$ ,  $a_2 = 0.94868$ , as an example of a 1G 1B 0L spectrum.



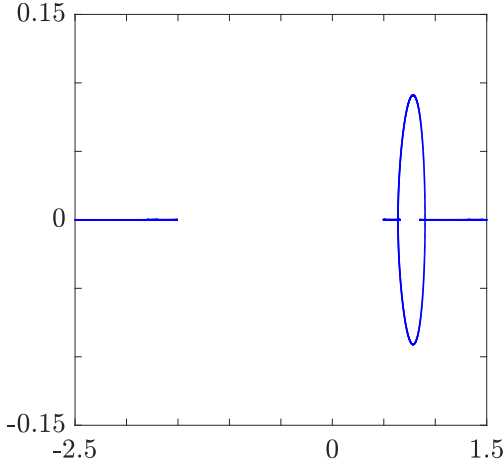
(d)  $\mathbf{S}_x$  for  $r = 15$ ,  $p = -13.45$ , *i.e.*,  $s_1 = 1$ ,  $s_2 = -1$ ,  $a_1 = 0.88034$ ,  $a_2 = 3.7716$ , as an example of a 1G 1B 1L spectrum.

Figure 3: Examples of spectra for different values of  $r$  and  $p$ , with  $q = 1$ .

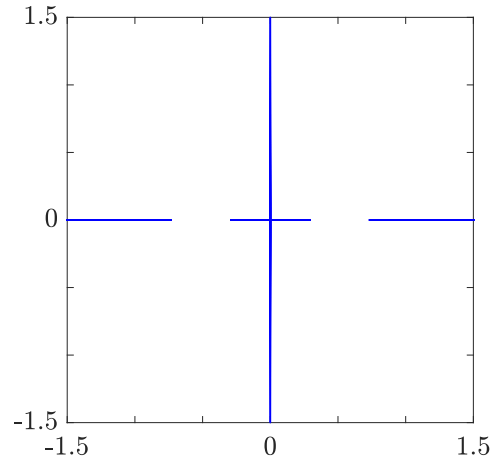
Once a solution  $u_1(x, t)$ ,  $u_2(x, t)$  has been fixed, the linearized equations (32) around this solution are

$$\begin{aligned} \delta u_{1t} &= i\{\delta u_{1xx} - 2[(2s_1|u_1|^2 + s_2|u_2|^2)\delta u_1 + s_1u_1^2\delta u_1^* + s_2u_1u_2^*\delta u_2 + s_2u_1u_2\delta u_2^*]\} \\ \delta u_{2t} &= i\{\delta u_{2xx} - 2[(s_1|u_1|^2 + 2s_2|u_2|^2)\delta u_2 + s_2u_2^2\delta u_2^* + s_1u_2u_1^*\delta u_1 + s_1u_2u_1\delta u_1^*]\}. \end{aligned} \quad (72)$$

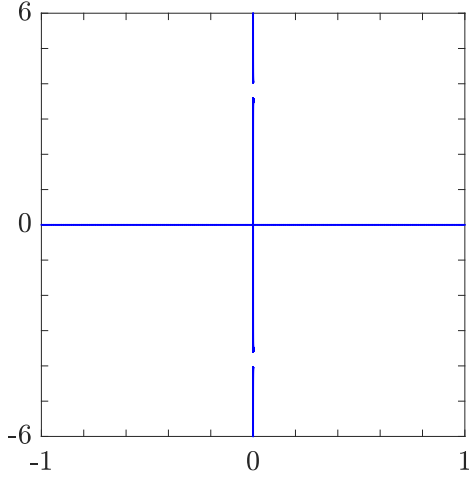
The two coupling constants  $s_1$ ,  $s_2$ , if non-vanishing, are just signs,  $s_1^2 = s_2^2 = 1$ , with no loss of generality. Thus the CNLS system (1) models three different processes, according to the defocusing or focusing self- and cross-interactions that each wave experiences. These different cases are referred to as (D/D) if  $s_1 = s_2 = 1$ , as (F/F) if  $s_1 = s_2 = -1$  and as (D/F) in the mixed case  $s_1s_2 = -1$ .



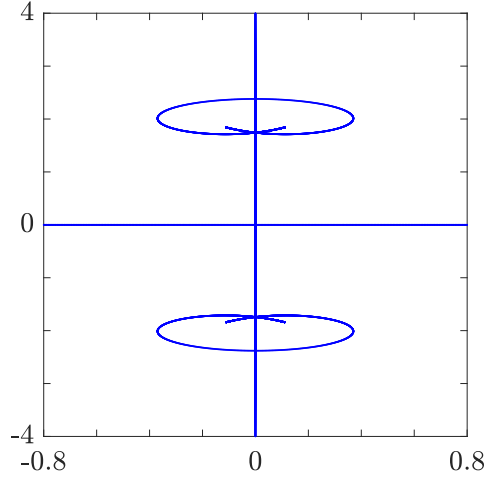
(e)  $\mathbf{S}_x$  for  $r = 1, p = 1.025$ , *i.e.*,  $s_1 = s_2 = 1$ ,  $a_1 = 1.0062, a_2 = 0.1118$ , as an example of a 2G 0B 1L spectrum.



(f)  $\mathbf{S}_x$  for  $r = 0, p = 0.1$ , *i.e.*,  $s_1 = s_2 = 1$ ,  $a_1 = a_2 = 0.22361$ , as an example of a degenerate case of a 2G 0B 1L spectrum: the imaginary axis in the spectrum is a loop passing through the point at infinity.



(g)  $\mathbf{S}_x$  for  $r = 0, p = -14$ , *i.e.*,  $s_1 = s_2 = -1, a_1 = a_2 = 2.6458$ , as an example of a degenerate case of a 0G 2B 0L spectrum: both branches are entirely contained on the imaginary axis; one branch passes through the point at infinity, whereas the other branch passes through the origin; for  $r = 0$ , two symmetrical gaps open on the imaginary axis for  $p \leq -8$ , as explained in [17].



(h)  $\mathbf{S}_x$  for  $r = 0, p = -4.7$ , *i.e.*,  $s_1 = s_2 = -1, a_1 = a_2 = 1.533$ , as an example of a degenerate case of a 0G 2B 0L spectrum: this case (which also appears in [31]) when projected back onto the stereographic sphere, can be completely explained in terms of the classification scheme provided in Proposition 9 (see [17]).

Figure 3 (Continued): Examples of spectra for different values of  $r$  and  $p$ , with  $q = 1$ .

Hereafter, our focus is on the stability of the CW solution (see (34), (35) with  $b_j = s_j a_j$ )

$$u_1(x, t) = a_1 e^{i(qx - \nu t)}, \quad u_2(x, t) = a_2 e^{-i(qx + \nu t)}, \quad \nu = q^2 + 2p, \quad (73)$$

where the parameter  $q$  is the relative wave number, which may be taken to be non negative  $q \geq 0$ , and  $a_1, a_2$  are the two amplitudes, whose values, with no loss of generality, may be real and non negative,  $a_j \geq 0$ . As for the notation, the parameter  $p$  is defined by (38a) which, in the present reduction, reads

$$p = s_1 a_1^2 + s_2 a_2^2. \quad (74a)$$

To make contact with the stability analysis presented in the two preceding sections, we introduce also the second relevant parameter  $r$  (38b) whose expression, in the present context, is

$$r = s_1 a_1^2 - s_2 a_2^2. \quad (74b)$$

At this point we show in Figure 4 the  $(r, p)$ -plane as divided in octants, according to different values of amplitudes and coupling constants.

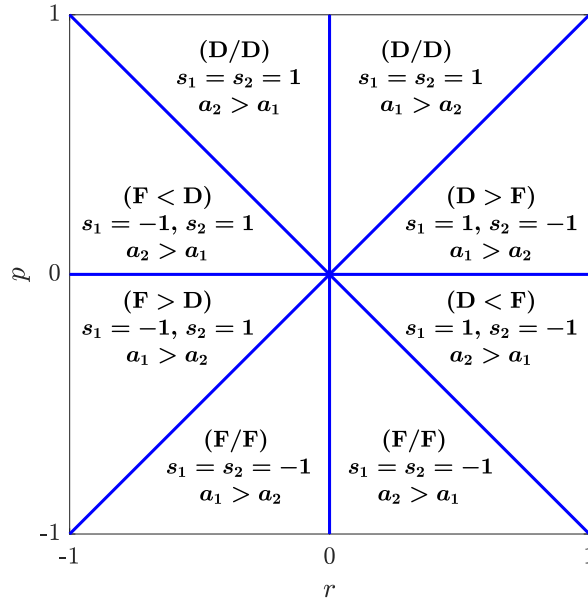


Figure 4: The  $(r, p)$ -plane divided according to amplitudes  $a_j$  and coupling constants  $s_j$ ,  $j = 1, 2$ .

We note that, as pointed out by Proposition 6, it is sufficient to confine our discussion to the half-plane  $r \geq 0$ , where four different experimental settings are represented, one in each of these four octants. These four states of two periodic waves can be identified either by the parameters  $p$  and  $r$  or by amplitudes and coupling constants according to the relations

$$s_1 a_1^2 = \frac{1}{2}(p + r), \quad s_2 a_2^2 = \frac{1}{2}(p - r), \quad (75)$$

each octant being characterized as shown in Figure 4. In particular the octant  $r > p > 0$  will be referred to as (D > F), whereas the octant  $-r < p < 0$  as (D < F), to indicate the wave with larger amplitude. Moreover, we observe again that setting  $q = 0$ , which characterizes two standing waves with equal wavelength, makes the stability properties of the CW solution very similar to that of the NLS equation. Indeed, in this case the solution (73) is stable if both waves propagate in a defocusing medium,  $s_1 = s_2 = 1$ , and

is unstable in the opposite case  $s_1 = s_2 = -1$ . However, this solution remains stable even if the wave  $u_2$  feels a self-focusing effect, *i.e.*  $s_2 = -1$ , provided the other wave  $u_1$  in the defocusing medium,  $s_1 = 1$ , has larger amplitude  $a_1 > a_2$ . Similarly, when  $q = 0$ , the CW solution is unstable if  $s_1 = 1$  and  $s_2 = -1$ , and if the larger amplitude wave is the one which propagates in the focusing medium,  $a_2 > a_1$ . These remarks follow from the explicit formulae (57) and (74a), and they are clearly evident in Figure 4 where, for  $r > 0$ , the upper two octants correspond to  $p > 0$ , and the lower two to  $p < 0$ .

The limit  $q \rightarrow 0$  of the results presented in the previous sections should be considered as formally singular. Indeed, the behavior of the CW (73) against small generic perturbations becomes significantly different from that reported above if the wave number mismatch  $2q$  is non vanishing. For one aspect, this is apparent from our first

**Remark 1** *If  $q \neq 0$ , then for no value of the amplitudes  $a_1, a_2$  with  $a_1 a_2 \neq 0$ , and for no value of the coupling constants  $s_1, s_2$ , the spectrum  $\mathbf{S}_x$  is entirely real.*

This follows from Proposition 9 and from our classification of the spectra in the parameter space into five types, all of which have a non-empty complex (non-real) component. The condition  $a_1 a_2 \neq 0$  for this statement to be true coincides with the condition that the point  $(r, p)$  neither belongs to the threshold curve  $p = p_+(r)$ , nor to the threshold curve  $p = p_-(r)$ , see (74). In particular, in the case  $p = r > 0$ , which is equivalent to setting  $a_2 = 0$  and  $s_1 = 1$ , the roots of  $P_W(w; \lambda)$ , (56), can be given in closed form,

$$w_1 = -(1/2)q + \sqrt{(\lambda + q/2)^2 - a_1^2}, \quad w_2 = -(1/2)q - \sqrt{(\lambda + q/2)^2 - a_1^2}, \quad w_3 = -\lambda + q,$$

so that

$$\begin{aligned} k_1 &= w_2 - w_3 = \lambda - \frac{3}{2}q - \sqrt{(\lambda + q/2)^2 - a_1^2}, \\ k_2 &= w_3 - w_1 = -\lambda + \frac{3}{2}q - \sqrt{(\lambda + q/2)^2 - a_1^2}, \\ k_3 &= w_1 - w_2 = 2\sqrt{(\lambda + q/2)^2 - a_1^2}, \end{aligned}$$

with the implication that  $\lambda$  has to be real to be in  $\mathbf{S}_x$ . In this case the spectrum is not immediately identifiable as one of the five types of spectra described in Proposition 9, for it corresponds to a threshold case between two of such types, and features one gap, no branches, and no loops. Moreover, this spectrum coincides with that obtained for the defocusing NLS equation via a Galilei transformation. In a similar fashion, if the point  $(r, p)$  is taken on the curve  $p = p_-(r)$ , namely  $p = -r < 0$  or, equivalently,  $a_1 = 0, s_2 = -1$ , the corresponding spectrum is that of the CW solution of the focusing NLS equation modulo a Galilei transformation, namely with no gap on the real axis, one branch on the imaginary axis, and no loop. Remark 1 has a straight implication on the stability of solution (73). This can be formulated as

**Remark 2** *If  $q a_1 a_2 \neq 0$  then the CW solution (73) is unstable.*

The relevant point here is the dependence on  $\lambda$  of the frequencies  $\omega_j(\lambda)$  over the spectrum  $\mathbf{S}_x$ . As we have shown in the previous section, if  $q a_1 a_2 \neq 0$ , the spectrum  $\mathbf{S}_x$  consists

of two components: one,  $\mathbf{RS}_x$ , is the real axis  $\text{Im}(\lambda) = 0$ , with possibly one or two gaps (see Proposition 8), and the second one,  $\mathbf{CS}_x$ , consists of branches and/or loops where  $\lambda$  runs off the real axis (see Proposition 9). Therefore the spectral representation (25) of the perturbation

$$\delta \mathbf{u} = \begin{pmatrix} \delta u_1 \\ \delta u_2 \end{pmatrix} \quad (76)$$

takes the form

$$\delta \mathbf{u} = e^{i(qx\sigma_3 - \nu t)} \left\{ \int_{\mathbf{RS}_x} d\lambda \sum_{j=1}^3 \left[ e^{i(xk_j - t\omega_j)} \mathbf{f}_+^{(j)}(\lambda) + e^{-i(xk_j - t\omega_j)} \mathbf{f}_-^{(j)}(\lambda) \right] + \int_{\mathbf{CS}_x} d\lambda \left[ e^{i(xk_3 - t\omega_3)} \mathbf{f}_+^{(3)}(\lambda) + e^{-i(xk_3 - t\omega_3)} \mathbf{f}_-^{(3)}(\lambda) \right] \right\}, \quad (77)$$

which is meant to separate the contribution to  $\delta \mathbf{u}$  due to the real part of the spectrum from that coming instead from the complex values of the integration variable  $\lambda$ , this being the integration over branches and loops. The 2-dim vector functions  $\mathbf{f}_\pm^{(j)}(\lambda)$  do not play a role here and are not specified. On the contrary, the reality property of the frequencies  $\omega_j$  over the spectrum is obviously essential to stability. Since the reality of the frequencies  $\omega_1, \omega_2, \omega_3$  for  $\lambda$  real has been proved in Proposition 5, it remains to show that indeed  $\omega_3(\lambda)$  is not real if  $\lambda$  belongs to branches or loops. This follows from the explicit expression (55), namely

$$\omega_3 = k_3(w_3 - \lambda) = \Omega + i\Gamma, \quad (78)$$

where  $k_3$  is real but  $w_3$  and  $\lambda$  cannot be real (see Section 3.2). Here the imaginary part  $\Gamma$  of  $\omega_3$  defines the *gain function* over the spectrum. This (possibly multivalued) function of  $k_3$  plays an important role in the initial stage of the unstable dynamics. Precisely, its dependence on the wave number  $k_3$  gives important information on the instability band and on time scales.

The physical interpretation is more transparent if these considerations are stated in terms of the amplitudes of the CW solution (73) for the three choices of the coupling constants  $s_1, s_2$  corresponding to integrable cases. In this respect, it is convenient to translate the classification of the spectra in the  $(a_1, a_2)$ -plane, in particular, and with no loss of generality, in the quadrant  $a_1 \geq 0, a_2 \geq 0$ . The four threshold curves  $p_\pm(r), p_S(r), p_C(r)$  which have been found in the  $(r, p)$ -plane, see Figure 2, are reproduced below in the  $(a_1, a_2)$ -plane, see Figure 5, according to the coordinate transformations (74) and (75). The outcome of this analysis is summarized by the following

**Proposition 10** *For each of the three integrable cases of the two coupled NLS equations (1) the spectrum is of the following types.*

(D/D)  $s_1 = s_2 = 1$  (see Figure 5a)

*The lower octant ( $a_1 \geq a_2$ ), which corresponds to  $r \geq 0$ , gets divided in two parts by the threshold curve  $p_S$  which intersects the line  $a_2 = a_1$  at the point  $(1/\sqrt{2}, 1/\sqrt{2})$ . In the lower, finite, part of this octant the spectrum  $\mathbf{S}_x$  is of type 2G 0B 1L, while in the other part it is of type 1G 1B 0L.*

(F/F)  $s_1 = s_2 = -1$  (see Figure 5b)

*The upper octant ( $a_2 \geq a_1$ ), which corresponds to  $r \geq 0$ , gets divided in two parts by*

the threshold curve  $p_C$  which intersects the line  $a_2 = a_1$  at the point  $(\sqrt{2}, \sqrt{2})$ . In the lower, finite, part of this octant the spectrum  $\mathbf{S}_x$  is of type 0G 2B 1L, while in the other part it is of type 0G 2B 0L.

(D/F)  $s_1 = 1, s_2 = -1$  (see Figure 5c)

The whole quadrant corresponds to  $r \geq 0$ . It is divided into three infinite portions by the two threshold curves  $p_C$ , in the upper octant, and  $p_S$  in the lower one. The spectrum is of type 1G 1B 1L in the upper part, it is of type 1G 1B 0L in the middle part, and of type 2G 0B 1L in the lower part.

These statements are straight consequences of Proposition 9 via the transformation (75).

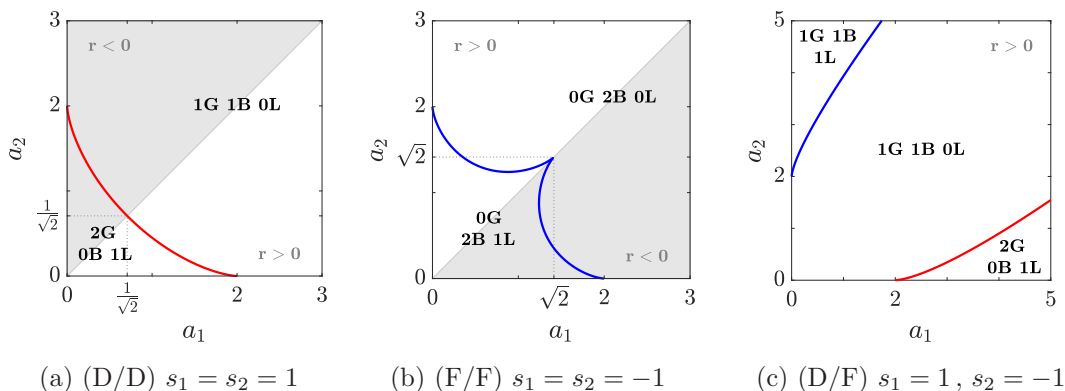


Figure 5: The  $(a_1, a_2)$ -plane (see Proposition 10).

We conclude by mentioning the limit case  $r = 0$ , see the end of the previous section. This concerns only the (D/D) and (F/F) cases of Proposition 9 and it coincides with the limit  $a_1 = a_2$ , namely with the case in which the two wave amplitudes are strictly equal. On this particular line of the  $(a_1, a_2)$ -plane, *i.e.*  $r = 0$  in the  $(r, p)$ -plane, the spectra are of four types, according to numbers of gaps, branches and loops, as it has been shortly discussed in Subsection 3.2.

## 4 Summary and conclusions

A sufficiently small perturbation of a solution of a (possibly multi-component) wave equation satisfies a linear equation. If the wave equation is integrable, the solution of this linear equation is formulated in terms of a set of eigenmodes whose expression is explicitly related to the solutions of the Lax pair. We give this connection in a general  $N \times N$  matrix formalism, which is local (in  $x$ ), and does not require specifying the boundary condition nor the machinery of the direct and inverse spectral problem. A by-product of our approach is the definition of the spectrum  $\mathbf{S}_x$ , associated to the unperturbed solution of the wave equation. It is worth stressing that the spectrum  $\mathbf{S}_x$  for  $N > 2$  does not coincide with the spectrum of the Lax equation  $\Psi_x = (i\lambda\Sigma + Q)\Psi$  in the complex  $\lambda$ -plane. This result is explicitly shown for  $N = 3$  in the instance of continuous wave solutions of two CNLS equations. In this case, we define as functions of  $\lambda$  on the spectrum  $\mathbf{S}_x$  the set of wave numbers  $k_j(\lambda)$  and frequencies  $\omega_j(\lambda)$  with the implication that the dispersion relation is

given in parametric form, the parameter being the spectral variable  $\lambda$  which appears in the Lax pair. In general, the spectrum is a complicate piecewise continuous curve. It obviously changes in the parameter space which is the set of values of the amplitudes of the two CWs, the mismatch  $q$  of their wave numbers, and the values of the coupling constants  $s_1, s_2$ . Apart from particular values of the parameters, the computation of the spectrum is not doable in analytic form, and has to be done numerically. The knowledge of the spectrum is sufficient to assess the stability of the CW solution. Generally, the spectrum consists of the real  $\lambda$ -axis with possibly one or two forbidden bands (gaps) and few additional finite curves which may be open (branches) or closed (loops). According to these topological properties, spectra can be classified in five different types to completely cover the entire parameter space. Only few marginal cases require separate consideration. Physically relevant information comes from the  $\lambda$  dependence of the eigenfrequency on branches and loops. In particular, one can read out of this dependence on  $\lambda$  the instability band and the time scale of the exponential growth in time of the perturbation. This is usually characterized by the imaginary part of the complex frequency, namely by the gain function. However, the investigation of this interesting aspect of the stability analysis is not reported here as it requires further analysis and computations. This part of our work will be reported elsewhere [17].

## A Structure of the gaps of the spectrum $\mathbf{S}_x$

The aim of this section is to provide additional details of the gap structure of the spectrum  $\mathbf{S}_x$  and to give a proof of Proposition 8 in Section 3.1, which states that the real part of the spectrum  $\mathbf{S}_x$  has either one, two or no gaps in the  $(r, p)$ -plane with  $r \geq 0$ . The no gap case occurs if the three eigenvalues  $w_j(\lambda)$  are real on the entire  $\lambda$ -axis. This happens if the discriminant (58) is positive for any real value of  $\lambda$ . By varying the value of  $p$  and/or  $r$  a gap may open up at the double zeros of the discriminant  $D_W(\lambda; q, p(\lambda), r)$ . Inside a gap the discriminant is negative and the three wave-numbers  $k_j(\lambda)$  (51) have a non vanishing imaginary part. We define implicitly the function  $p \equiv p(\lambda)$  as those values of the parameter  $p$  such that the discriminant  $D_W(\lambda; q, p(\lambda), r) = 0$ .

In order to compute the number of gaps from the expression (58) of the discriminant  $D_W(\lambda; q, p, r)$ , we plot  $p(\lambda)$  as a function of  $\lambda$  real, for few fixed values of  $r$ , and  $q = 1$ . Four such plots of  $p(\lambda)$  are shown in Figure 6 for four different values of  $r$ . The intersections of this plotted curve with the straight line corresponding to a constant value of  $p$  provide the endpoints of those gaps which occur at the given value of  $p$  (and at the fixed values of  $r$  and  $q$ ). For instance, the analytical results presented above for  $r = 0$ , see Proposition 7, can be clearly read out of the left plot in Figure 6a. The two local minima at  $\lambda = \pm 0.5, p = 0$  show the opening of the two gaps that we have analytically found for  $0 < p < 1$ . For future reference, we also note that the local maximum of  $p(\lambda)$  is taken at  $\lambda = \lambda_S = 0$ , namely  $p(\lambda_S) = p_S = 1$ , and that the function  $p(\lambda)$  has a cusp (a double singular point), namely is not analytic, at  $\lambda_S$ . If the parameter  $r$  increases,  $r > 0$ , this plot gets asymmetrically deformed as shown in Figures 6b, 6c and 6d. Figure 6b shows that no gap exists for  $p < -r = -0.5$ , while for  $-0.5 = -r < p < r = 0.5$  only one gap occurs. Instead, for  $0.5 = r < p < p_S$  two distinct gaps appear. Finally, for  $p_S < p < +\infty$  again only one gap is present. As in the previous plot, here  $p_S$  denotes the local maximum and singular point

of  $p(\lambda)$ . Moreover, we observe that this graph is consistent with the following alternative expression of the discriminant (58) for  $p = -r$ ,

$$D_W(\lambda, q, -r, r) = (4q\lambda + 2q^2 - r)^2[(2\lambda - q)^2 + 4r],$$

which is clearly positive definite for any non negative  $r$ , and any real  $\lambda$  with the exception of  $\lambda = \frac{r}{4q} - \frac{q}{2}$  where  $p(\lambda)$  takes its minimum value.

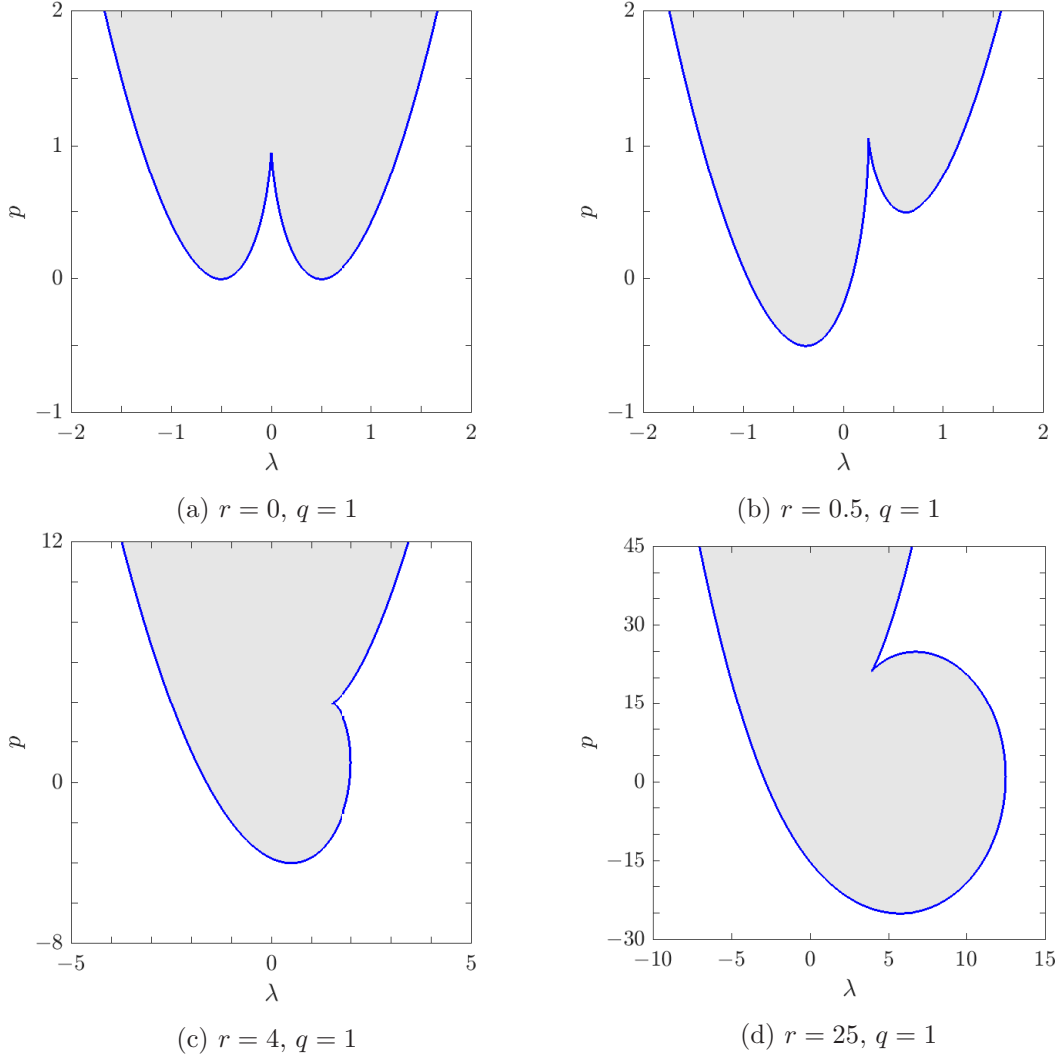


Figure 6:  $p(\lambda)$  defined by  $D_W(\lambda; q, p(\lambda), r) = 0$ ; the grey area corresponds to  $D_W < 0$ .

By increasing further the value of  $r$ , Figure 6b changes and eventually looks different as the local maximum  $p_S$  becomes a local minimum. The transition is illustrated in Figure 6c computed at  $r = 4$ , with  $q = 1$ . After the transition, the curve  $p(\lambda)$  takes the form shown in Figure 6d computed at  $r = 25$ , with  $q = 1$ . Again,  $p = -r$  is still the minimum of  $p(\lambda)$  while  $p = r$  is instead a local maximum. The singularity at  $\lambda = \lambda_S$  is such that now  $p_S = p(\lambda_S)$  is a local minimum with  $p_S < r$ . Indeed,  $\lambda_S$  is the only singularity of  $p(\lambda)$  and its dependence on the parameter  $r$ ,  $\lambda_S = \lambda_S(r)$ , is implicitly expressed by its inverse relation  $r = r(\lambda_S)$ ,

$$r = 2\frac{\lambda_S}{q} \left( q^2 + \frac{4}{27}\lambda_S^2 \right). \quad (\text{A.1})$$

This yields a one-to-one correspondence between any non negative real  $r$  and a real  $\lambda_S(r)$  since we prove that, for any  $r \geq 0$ , the cubic equation (A.1) has two complex conjugate roots. Moreover, we find also the following useful relations associated with the singular value  $\lambda_S$ :

$$p_S = q^2 + \frac{4}{3}\lambda_S^2; \quad w_j = -\frac{1}{3}\lambda_S, \quad z_j = -q^2 + \frac{2}{9}\lambda_S^2, \quad k_j = \omega_j = 0, \quad j = 1, 2, 3. \quad (\text{A.2})$$

The transition between the two regimes with  $p_S(r) > r$  and  $p_S(r) < r$  takes place at the special threshold value  $r = r_T$ , where  $p_S(r_T) = r_T$ . With self-evident notation, we find that

$$r_T = p_T = p_S(r_T) = 4q^2, \quad \lambda_T = \frac{3}{2}q. \quad (\text{A.3})$$

The implicit expressions of  $\lambda_S(r)$  (A.1) is made explicit in (61). The function  $p_S(r)$  is plotted in Figure 1.

## B Analysis of the $x$ -spectrum

As pointed out in Section 3.2, the nature and the number of the components of the  $x$ -spectrum  $\mathbf{S}_x$ , seen as a curve in the  $\lambda$ -plane, are classified by the number of sign-changes of the discriminant of  $\mathcal{P}(\zeta; \lambda, q, p, r)$  with respect to  $\lambda$ , *i.e.*  $\Delta_\lambda \mathcal{P}(\zeta; \lambda, q, p, r) = \mathcal{Q}(\zeta; q, p, r)$ , for  $\zeta \geq 0$  (see also (B.1a) in the following). The aim of this section is to give details of this result. Without loss of generality, from now on we will assume  $q = 1$ .

Given the (cubic) polynomial  $P_W(w; \lambda, q, p, r)$ , we would like to describe the geometrical locus in the  $\lambda$ -plane constituted by the complex values of  $\lambda$  such that, for each value of  $\lambda$  in the locus, the polynomial  $P_W(w; \lambda, q, p, r)$  has at least two  $w$ -roots such that their difference is real. As discussed in Section 3.2, since we are interested in the differences of the roots, it is convenient to introduce the polynomial  $\mathcal{P}(\zeta; \lambda, q, p, r)$ , see (64), whose  $\zeta$ -roots are the squares of the differences of the original  $w$ -roots of  $P_W(w; \lambda, q, p, r)$ . The polynomial  $\mathcal{P}(\zeta; \lambda, q, p, r)$  can be conveniently re-written as

$$\mathcal{P}(\zeta; \lambda, q, p, r) = \begin{pmatrix} 1 & \lambda & \lambda^2 & \lambda^3 & \lambda^4 \end{pmatrix} \cdot \Pi \cdot \begin{pmatrix} 1 \\ \zeta \\ \zeta^2 \\ \zeta^3 \end{pmatrix}$$

with

$$\Pi \equiv \Pi(p, r) = \begin{pmatrix} 4(p-1)^3 + 27r^2 & 9(p-1)^2 & 6(p-1) & 1 \\ -36(p+2)r & 0 & 0 & 0 \\ 4(8+20p-p^2) & -24(p-1) & -8 & 0 \\ 32r & 0 & 0 & 0 \\ -64 & 16 & 0 & 0 \end{pmatrix}.$$

Observe that  $\zeta = k_j^2$  for some  $j$ . As in Section 3.2, let  $j = 3$ . The polynomial  $\mathcal{P}(\zeta; \lambda, q, p, r)$  can be regarded as a 3<sup>rd</sup> degree polynomial in  $\zeta$ , as well as a 4<sup>th</sup> degree polynomial in  $\lambda$ . Hence our problem translates into finding the complex values of  $\lambda$  for which  $\mathcal{P}(\zeta; \lambda, q, p, r)$ , seen as a polynomial in  $\zeta$ , admits at least one real, positive root  $\zeta = k_3^2$ . The  $x$ -spectrum

$\mathbf{S}_x$  then coincides with the locus of the roots of  $\mathcal{P}(\zeta; \lambda, q, p, r)$  regarded as a polynomial in  $\lambda$  for all values of  $\zeta > 0$ , namely for  $\zeta$  considered as a real, positive parameter.

From the algebraic-geometric point of view, the locus of the roots of  $\mathcal{P}(\zeta; \lambda, q, p, r)$  in the  $\lambda$ -plane is an algebraic curve; this can be given explicitly as a system of two polynomial equations in two unknowns by setting  $\lambda = \mu + i\rho$  and then separating the real and the imaginary parts of  $\mathcal{P}(\zeta; \lambda, q, p, r)$ . In the following we will apply Sturm's chains (*e.g.*, see [18, 23]) on  $\mathcal{Q}(\zeta; q, p, r)$ , the discriminant of  $\mathcal{P}(\zeta; \lambda, q, p, r)$ , and invoke Sturm's theorem to study its roots, in order to obtain a classification of the different loci  $\mathbf{S}_x$ .

## B.1 Sturm chains and spectra classification in the $(r, p)$ -plane

Let  $P(x)$  be a polynomial in  $x$  with real coefficients, and let  $\deg(P)$  be its degree. A Sturm's chain [18, 23]

$$\begin{aligned} P^{(0)}(x) &= P(x), \\ P^{(1)}(x) &= \frac{d}{dx}P^{(0)}(x) \\ P^{(2)}(x) &= -\text{Remainder}(P^{(0)}(x), P^{(1)}(x)), \\ &\vdots \\ P^{(j)}(x) &= -\text{Remainder}(P^{(j-2)}(x), P^{(j-1)}(x)), \end{aligned}$$

is a sequence of polynomials associated with a given polynomial  $P(x)$ , and its derivative, where the notation  $\text{Remainder}(P_1, P_2)$  stands for the remainder of the polynomial division between  $P_1$  and  $P_2$ . By Sturm's theorem the sequence allows to find the number of distinct real roots of  $P(x)$ , in a given interval, in terms of the number of changes of signs of the values of the Sturm sequence at the end points of the interval, which can even be taken to be  $\pm\infty$ . When applied to the whole real line, it gives the total number of real roots of  $P(x)$ . Since  $\deg(P^{(i+1)}) < \deg(P^{(i)})$  for  $0 \leq i < j$ , the algorithm terminates and it contains in general  $\deg(P) + 1$  polynomials. The final polynomial,  $P^{(j)}(x)$ , is the greatest common divisor of  $P(x)$  and its derivative. For instance, suppose that we would like to find the number of distinct real roots of  $P(x)$  in the real interval  $[x_i, x_f]$ ; let  $\varsigma(x_i)$  and  $\varsigma(x_f)$  be the number of changes of sign of the Sturm chain at  $x_i$  and  $x_f$ , respectively; then, Sturm's theorem states that the number of real roots of  $P(x)$  in  $[x_i, x_f]$  is simply given by  $\varsigma(x_i) - \varsigma(x_f)$ .

For each value of  $\zeta > 0$ , we have four values of  $\lambda$ , as  $\mathcal{P}(\zeta; \lambda, q, p, r)$  is a 4<sup>th</sup> degree polynomial in  $\lambda$ . For all  $p, r$  real, there always exist four values of  $\lambda$  such that  $P_W(w; \lambda, q, p, r)$  has at least one double  $w$ -root. The nature of these four points can be classified in terms of the sign of  $\Delta_\lambda \Delta_w P_W(w; \lambda, q, p, r)$ . Observe that  $\mathcal{P}(0; \lambda, q, p, r)$  coincides with  $\Delta_\lambda P_W(w; \lambda, q, p, r)$ , the discriminant of  $P_W(w; \lambda, q, p, r)$  with respect to  $\lambda$ , with reversed sign. Furthermore, the discriminant of  $\mathcal{P}(0; \lambda, q, p, r)$  with respect to  $\lambda$ ,  $\Delta_\lambda \mathcal{P}(0; \lambda, q, p, r)$ , coincides with  $\Delta_\lambda \Delta_w P_W(w; \lambda, q, p, r)$ . Thus, a first classification of  $\mathbf{S}_x$  can be achieved by imposing

$$\Delta_\lambda \mathcal{P}(0; \lambda, q, p, r) = -1048576 (p - r) (p + r) [(p - 1) (p + 8)^2 - 27 r^2]^3 = 0,$$

see Proposition 8.

In order to obtain a complete classification of  $\mathbf{S}_x$  for all  $\zeta$ , we observe that, by moving  $\zeta$  in the interval  $(0, +\infty)$ , we move the four  $\lambda$ -roots of the polynomial  $\mathcal{P}(\zeta; \lambda, q, p, r)$  (regarded as a polynomial in  $\lambda$ ). Two of such roots will collide if  $\Delta_\lambda \mathcal{P}(\zeta; \lambda, q, p, r) = \mathcal{Q}(\zeta; q, p, r) \equiv \mathcal{Q}(\zeta)$  vanishes. Since

$$\Delta_\lambda \mathcal{P}(\zeta; \lambda, q, p, r) = \mathcal{Q}(\zeta) = 65536 \mathcal{Q}_1^2(\zeta) \mathcal{Q}_2(\zeta), \quad (\text{B.1a})$$

$$\mathcal{Q}_1(\zeta) = p^3 - 27r^2 - 3p^2(\zeta - 5) - 12p(\zeta - 4) + 4(\zeta - 1)(\zeta - 4)^2, \quad (\text{B.1b})$$

$$\begin{aligned} \mathcal{Q}_2(\zeta) = & 4p^5(\zeta - 4) + p^4(\zeta - 4)(\zeta + 60) + 16p^3(3\zeta^2 + r^2 - 48) + \\ & + 8p^2[\zeta(\zeta - 4)(\zeta + 36) - 32(\zeta - 4) + r^2(84 - 15\zeta)] + \\ & + 32p[4\zeta(\zeta - 4)(\zeta - 2) - 3r^2\zeta(\zeta - 4) + 24r^2] + \\ & + 16[\zeta^2(\zeta - 4)^2 - r^2(\zeta - 8)(\zeta - 2)(\zeta + 4) - 27r^4], \end{aligned} \quad (\text{B.1c})$$

and, because  $\mathcal{Q}_1(\zeta)$  appears squared in the expression of  $\mathcal{Q}(\zeta)$ , the sign of  $\mathcal{Q}(\zeta)$  depends solely on the sign of  $\mathcal{Q}_2(\zeta)$ . Moreover, we observe that the real, positive roots of  $\mathcal{Q}_1(\zeta)$  are not associated to any change in the behaviour of  $\lambda$ , as  $\mathcal{Q}(\zeta)$  does not change sign if  $\zeta$  passes through one of those roots: indeed, if  $\zeta$  passes through one of the roots of  $\mathcal{Q}_1(\zeta)$ , then two  $\lambda$ -roots will collide, but after the collision they will remain on the branches that they occupied before the collision.

It is easy to see, by isolating the leading term in  $\zeta$  of  $\mathcal{Q}(\zeta)$ , that  $\mathcal{Q}(\zeta) > 0$  for large  $\zeta$ . In particular, all the  $\lambda$ -roots of  $\mathcal{P}(\zeta; \lambda, q, p, r)$  are real if  $\zeta$  is larger than the maximum of the real, positive roots of  $\mathcal{Q}_2(\zeta)$ . After that point there are no complex branches in the  $\lambda$ -plane, and this provides a simple limit for the largest value of  $k_3 = \sqrt{\zeta}$  for which the gain function is defined (see (78)). This also proves that the real axis or part of it is always included in the locus on the  $\lambda$ -plane. On the other hand, if  $\mathcal{Q}(\zeta) < 0$ , then two of the  $\lambda$  roots are real and two of the  $\lambda$ -roots form a pair of complex conjugate values. By changing the value of  $\zeta$  and keeping  $\mathcal{Q}(\zeta)$  negative, two of the  $\lambda$ -roots will move on the real axis and other two will move in the complex plane. When  $\mathcal{Q}(\zeta) = 0$ , then two of the  $\lambda$ -roots collide in one point. Finally, if  $\mathcal{Q}(\zeta) > 0$  for  $\zeta > 0$  and smaller than the maximum of the real roots of  $\mathcal{Q}_2(\zeta)$ , we can have either four real roots or two pairs of complex conjugate roots.

Based on what we have seen so far, it is clear that the structure of the algebraic curves in the  $\lambda$ -plane (*i.e.* the  $x$ -spectrum  $\mathbf{S}_x$ ) is related to the number of changes of sign of  $\mathcal{Q}(\zeta)$  for  $\zeta \geq 0$ , that is the number of changes of sign of  $\mathcal{Q}_2(\zeta)$  for  $\zeta \geq 0$ . In turn, as one varies  $p$  and  $r$ , the number of changes of sign of  $\mathcal{Q}_2(\zeta)$  for  $\zeta \geq 0$  can be obtained by counting the number of positive roots of  $\mathcal{Q}_2(\zeta)$ . In particular, as  $p$  and  $r$  vary, the number of positive roots of  $\mathcal{Q}_2(\zeta)$  changes in two possible ways: either two roots collide on the real  $\zeta$  axis and then move onto the complex plane as a pair of complex conjugate roots (or viceversa), or a positive root passes through the origin and becomes negative (or viceversa). Therefore, in order to provide a complete classification of all the algebraic curves (*i.e.*, the spectra) in the  $\lambda$ -plane, not only we need to understand the number of changes of sign of  $\mathcal{Q}_2(\zeta)$  for  $\zeta \geq 0$  (which is the number of its positive zeros), but also the general structure of the zeros of  $\mathcal{Q}_2(\zeta)$  (namely, the nature of the its non-positive roots).

To this end we compute the Sturm chain  $\{\mathcal{Q}_2^{(j)}\}_{j=0}^4 = \{\mathcal{Q}_2^{(0)}, \mathcal{Q}_2^{(1)}, \mathcal{Q}_2^{(2)}, \mathcal{Q}_2^{(3)}, \mathcal{Q}_2^{(4)}\}$  of  $\mathcal{Q}_2(\zeta)$  at  $\zeta = 0$  and the leading terms of the Sturm chain as  $\zeta \rightarrow +\infty$ , with

$$\begin{aligned}\mathcal{Q}_2^{(0)}(\zeta) &= \mathcal{Q}_2(\zeta), \\ \mathcal{Q}_2^{(1)}(\zeta) &= \frac{d}{d\zeta}\mathcal{Q}_2^{(0)}(\zeta), \\ \mathcal{Q}_2^{(2)}(\zeta) &= -\text{Remainder}\left(\mathcal{Q}_2^{(0)}(\zeta), \mathcal{Q}_2^{(1)}(\zeta)\right), \\ \mathcal{Q}_2^{(3)}(\zeta) &= -\text{Remainder}\left(\mathcal{Q}_2^{(1)}(\zeta), \mathcal{Q}_2^{(2)}(\zeta)\right), \\ \mathcal{Q}_2^{(4)}(\zeta) &= -\text{Remainder}\left(\mathcal{Q}_2^{(2)}(\zeta), \mathcal{Q}_2^{(3)}(\zeta)\right).\end{aligned}$$

Because of the parametric dependence on  $p$  and  $r$ , the expressions of these quantities are rather large and we prefer not to write the terms of the sequence explicitly here. Just to give the reader an idea, the constant term of the sequence reads

$$\mathcal{Q}_2^{(4)}(\zeta) = -\frac{\text{Num}(\mathcal{Q}_2^{(4)})}{\text{Den}(\mathcal{Q}_2^{(4)})}$$

with  $\text{Num}(\mathcal{Q}_2^{(4)})$  equal to

$$r^2(-p+r)(p+r)(256+160p^2+p^4-12p^2r^2+12r^4)^2(4096-768p^2+48p^4-p^6-432p^2r^2+432r^4)^3$$

and  $\text{Den}(\mathcal{Q}_2^{(4)})$  equal to

$$\begin{aligned}4(1048576p^2 - 262144p^4 + 24576p^6 - 1024p^8 + 16p^{10} + 4063232p^2r^2 + 126976p^4r^2 + \\ - 8448p^6r^2 - 944p^8r^2 - p^{10}r^2 4063232r^4 - 126976p^2r^4 + 77568p^4r^4 + 4400p^6r^4 + p^8r^4 + \\ - 138240p^2r^6 - 6912p^4r^6 + 69120r^8 + 3456p^2r^8)^2.\end{aligned}$$

If  $\varsigma(0)$  is the number of changes of sign for the Sturm chain  $\{\mathcal{Q}_2^{(j)}\}_{j=0}^4$  at  $\zeta = 0$  and  $\varsigma(\infty)$  the number of changes of sign of the leading terms of the Sturm chain as  $\zeta \rightarrow +\infty$ , then, by Sturm's theorem, the number of positive roots of  $\mathcal{Q}_2(\zeta)$  is simply given by  $\varsigma(0) - \varsigma(\infty)$ . Using this approach, we obtain that, for all  $r, p$  real,  $\mathcal{Q}_2(\zeta)$  has always at least one real, positive root. Moreover, in this way we obtain a set of ten algebraic curves in the  $(r, p)$ -plane, whose intersection defines a set of regions where either  $\varsigma(0)$ , or  $\varsigma(\infty)$ , or both change value, namely where the structure of the zeros of  $\mathcal{Q}_2(\zeta)$  is expected to vary.

Finally, by checking carefully each one of these regions and using some elementary, classical invariant theory [37], after a long and tedious analysis, we verify that the following four curves (see (62), (63), and (69))

$$\begin{aligned}p - r &= 0, \\ p + r &= 0, \\ (p - 1)(p + 8)^2 - 27r^2 &= 0, \quad p = p_S(r), \\ (p^2 - 16)^3 + 432r^2(p^2 - r^2) &= 0, \quad p = p_C(r), \quad \text{with } p < 0,\end{aligned}$$

determine the regions where  $\mathcal{Q}_2(\zeta)$  changes the number of positive and negative roots, and hence the structure of its roots. In particular we have the following

**Proposition 11** For  $r \geq 0$  and  $q = 1$ , the polynomial  $Q_2(\zeta; q, r, p)$  has the following structure of zeros.

If  $r < 4$

$-\infty < p < p_C(r)$	2 positive, 0 negative, and 2 complex conjugate roots
$p_C(r) < p < -r$	4 positive, 0 negative, and 0 complex conjugate roots
$-r < p < r$	1 positive, 1 negative, and 2 complex conjugate roots
$r < p < p_S(r)$	2 positive, 2 negative, and 0 complex conjugate roots
$p_S(r) < p < +\infty$	1 positive, 1 negative, and 2 complex conjugate roots

If  $r > 4$

$-\infty < p < -r$	2 positive, 0 negative, and 2 complex conjugate roots
$-r < p < p_C(r)$	3 positive, 1 negative, and 0 complex conjugate roots
$p_C(r) < p < p_S(r)$	1 positive, 1 negative, and 2 complex conjugate roots
$p_S(r) < p < r$	2 positive, 2 negative, and 0 complex conjugate roots
$r < p < +\infty$	1 positive, 1 negative, and 2 complex conjugate roots

At the threshold values, either  $Q_2(\zeta; q, r, p)$  features a double root, or a positive root passes through the origin.

It is not difficult to verify that, for  $q = 1$ , when  $Q_2(\zeta; q, r, p)$  has 2 positive, 0 negative, and 2 complex conjugate roots, then  $\mathbf{S}_x$  has 0 gaps, 2 branches, and 0 loops (0G 2B 0L); when  $Q_2(\zeta; q, r, p)$  has 4 positive, 0 negative, and 0 complex conjugate roots, then  $\mathbf{S}_x$  has 0 gaps, 2 branches, and 1 loop (0G 2B 1L); when  $Q_2(\zeta; q, r, p)$  has 4 positive, 0 negative, and 0 complex conjugate roots, then  $\mathbf{S}_x$  has 1 gap, 1 branch, and 0 loops (1G 1B 0L); when  $Q_2(\zeta; q, r, p)$  has 3 positive, 1 negative, and 0 complex conjugate roots, then  $\mathbf{S}_x$  has 1 gap, 1 branch, and 1 loop (1G 1B 1L); when  $Q_2(\zeta; q, r, p)$  has 2 positive, 2 negative, and 0 complex conjugate roots, then  $\mathbf{S}_x$  has 2 gaps, 0 branches, and 1 loop (2G 0B 1L). Consequently, the four curves (62), (63), and (69) determine the regions where the number and the nature of the components of the algebraic curve  $\mathbf{S}_x$  change. The regions are those described in Proposition 9 and reported in Figure 2 in Section 3.2.

## C Numerical computation of the spectra

In this section we briefly illustrate how the spectra can be computed numerically. Let  $\hat{\zeta}_j \geq 0$ ,  $j = 1, \dots, \hat{n}$ , with  $1 \leq \hat{n} \leq 4$ , be the real, positive roots of the polynomial  $Q_2(\zeta)$  (B.1c). We recall that  $Q_2(\zeta)$  has always at least one real, positive root. Moreover, the non-real part of the spectrum  $\mathbf{S}_x$  is the locus on the  $\lambda$ -plane of the  $\lambda$ -roots of  $\mathcal{P}(\zeta; \lambda, q, p, r)$  for  $0 \leq \zeta \leq \max_j \hat{\zeta}_j$ . Thus, to numerically compute a spectrum for a given choice of  $r$  and  $p$ , with  $q = 1$ , it suffices to solve  $\mathcal{P}(\zeta; \lambda, q, p, r) = 0$  for the same choice of the parameters, for a convenient set of values of  $\zeta$  in the interval  $[0, \max_j \hat{\zeta}_j]$ . These values will be referred to as  $\zeta$ -nodes. As zeros of  $Q_2(\zeta)$  are zeros of the discriminant of  $\mathcal{P}(\zeta; \lambda, q, p, r)$ , with respect

to  $\lambda$ , we expect that when  $\zeta$  is close to one of the  $\hat{\zeta}_j$ 's the algebraic curve  $\mathbf{S}_x$  undergoes rapid changes. This implies that in order to capture all features of the spectrum, and optimize the root-extracting procedure, it is expedient to distribute the  $\zeta$ -nodes according to a Chebyshev-Gauss-Lobatto distribution [36] between each one of the intervals  $[0, \hat{\zeta}_1]$ ,  $[\hat{\zeta}_1, \hat{\zeta}_2], \dots, [\hat{\zeta}_{\hat{n}-1}, \hat{\zeta}_{\hat{n}}]$ .

The simultaneous computation of all the roots of all polynomials has been performed via the standard technique of evaluating the eigenvalues of a companion matrix, as per implemented in MATLAB R2017a. Note also that all spectra have been verified using an objective-function technique over the imaginary part of the differences of the  $w_j$ 's, computed by solving directly  $P_W(\zeta; \lambda, q, p, r) = 0$ .

## References

- [1] M.J. Ablowitz and P.A. Clarkson. *Solitons, Nonlinear Evolution Equations and Inverse Scattering*. London Mathematical Society Lecture Note Series. Cambridge University Press, 1991.
- [2] M.J. Ablowitz and T.P. Horikis. Interacting nonlinear wave envelopes and rogue wave formation in deep water. *Physics of Fluids*, 27(1):012107, 2015.
- [3] M.J. Ablowitz, D.J. Kaup, A.C. Newell, and H. Segur. The inverse scattering transform-fourier analysis for nonlinear problems. *Studies in Applied Mathematics*, 53(4):249–315, 1974.
- [4] M.J. Ablowitz and H. Segur. *Solitons and the Inverse Scattering Transform*. Studies in Applied Mathematics. SIAM, 1981.
- [5] G.P. Agrawal. *Nonlinear Fiber Optics*. Academic Press, 1995.
- [6] F. Baronio, M. Conforti, A. Degasperis, S. Lombardo, M. Onorato, and S. Wabnitz. Vector Rogue Waves and Baseband Modulation Instability in the Defocusing Regime. *Phys. Rev. Lett.*, 113:034101, 2014.
- [7] T.B. Benjamin and J.E. Feir. The disintegration of wave trains on deep water Part 1. Theory. *Journal of Fluid Mechanics*, 27:417–430, 1967.
- [8] G. Biondini and D. Mantzavinos. Universal nature of the nonlinear stage of modulational instability. *Phys. Rev. Lett.*, 116(4):043902, 2016.
- [9] N. Bottman, D. Deconinck, and M. Nivala. Elliptic solutions of the defocusing NLS equation are stable. *J. Phys. A: Math. Theor.*, 44:285201, 2009.
- [10] F. Calogero and A. Degasperis. *Spectral Transform and Solitons: Tools to Solve and Investigate Nonlinear Evolution Equations. V. 1*. North-Holland, 1982.
- [11] F. Calogero and A. Degasperis. New Integrable Equations of Nonlinear Schrödinger Type. *Studies in Applied Mathematics*, 113(1):91–137, 2004.
- [12] T. Dauxois and M. Peyrard. *Physics of Solitons*. Cambridge University Press, 2006.

- [13] A. Degasperis. Integrable nonlocal wave interaction models. *J. Phys. A: Math. Theor.*, 44(5):052002, 2011.
- [14] A. Degasperis and S. Lombardo. Multicomponent integrable wave equations. Darboux-Dressing transformation. *J. Phys. A: Math. Theor.*, 40(5):961–977, 2007.
- [15] A. Degasperis and S. Lombardo. Multicomponent integrable wave equations. Soliton solutions. *J. Phys. A: Math. Theor.*, 42(38):385206, 2009.
- [16] A. Degasperis and S. Lombardo. Integrability in action: Solitons, instability and rogue waves. In M. Onorato, S. Resitori, and F. Baronio, editors, *Rogue and Shock Waves in Nonlinear Dispersive Media*, pages 23–53. Springer, 2016.
- [17] A. Degasperis, S. Lombardo, and M. Sommacal. Coupled nonlinear Schrödinger equations: spectra and instabilities of plane waves. in preparation, 2017.
- [18] B.P. Demidovich and I.A. Maron. *Computational Mathematics*. Mir Publishers, 1981.
- [19] R.K. Dodd, J.C. Eilbeck, J.D. Gibbon, and H.C. Morris. *Solitons and nonlinear wave equations*. Academic Press, 1982.
- [20] Jr.S.G. Evangelides, L.F. Mollenauer, J.P. Gordon, and N.S. Bergano. Polarization multiplexing with solitons. *Lightwave Technology, Journal of*, 10(1):28–35, 1992.
- [21] M.G. Forest, D.W. McLaughlin, D.J. Muraki, and O.C. Wright. Nonfocusing instabilities in coupled, integrable nonlinear Schrödinger PDEs. *Journal of Nonlinear Science*, 10(3):291–331, 2000.
- [22] H. Hasimoto and H. Ono. Nonlinear Modulation of Gravity Waves. *Journal of the Physical Society of Japan*, 33:805–811, September 1972.
- [23] D.G. Hook and P.R. McAree. Using Sturm Sequences to Bracket Real Roots of Polynomial Equations. In Andrew S. Glassner, editor, *Graphics Gems*, pages 416–422. Academic Press, 1990.
- [24] D.J. Kaup. Closure of the squared Zakharov-Shabat eigenstates. *J. Math. Anal. Appl.*, 54:849–864, 1976.
- [25] D.J. Kaup. The Three-Wave Interaction – A Nondispersive Phenomenon. *Studies in Applied Mathematics*, 55(1):9–44, 1976.
- [26] P.G. Kevrekidis, D.J. Frantzeskakis, and R. Carretero-González. *Emergent Nonlinear Phenomena in Bose-Einstein Condensates: Theory and Experiment*. Springer Series on Atomic, Optical, and Plasma Physics. Springer, 2007.
- [27] E.A. Kuznetsov. Solitons in a parametrically unstable plasma. *Dokl. Akad. Nauk SSSR*, 236(9):575–577, 1977.
- [28] E.A. Kuznetsov and A.V. Mikhailov. Stability of stationary waves in nonlinear weakly dispersive media. *Zh. Eksp. Teor. Fiz.*, 67:1717–1727, 1974.
- [29] E.A. Kuznetsov and M.D. Spector. Modulation instability of soliton trains in fiber communication systems. *Theor. Math. Phys.*, 120(2):997–1008, 1999.

- [30] E.A. Kuznetsov, M.D. Spector, and Fal'kovich. On the stability of nonlinear waves in integrable models. *Physica D*, 10:379–386, 1984.
- [31] L. Ling and L.C. Zhao. Modulational instability and homoclinic orbit solutions in vector nonlinear schrödinger equation. preprint arXiv:1704.00404.
- [32] S.V. Manakov. On the theory of two-dimensional stationary self-focusing of electromagnetic waves. *Soviet Journal of Experimental and Theoretical Physics*, 38, 1974.
- [33] C. Menyuk. Nonlinear pulse propagation in birefringent optical fibers. *IEEE Journal of Quantum Electronics*, 23(2):174–176, Feb 1987.
- [34] S.P. Novikov, S.V. Manakov, L.P. Pitaevskii, and V.E. Zakharov. *Theory of Solitons: The Inverse Scattering Method*. Contemporary Soviet Mathematics. Plenum, 1984.
- [35] M. Onorato, D. Proment, and A. Toffoli. Freak waves in crossing seas. *The European Physical Journal Special Topics*, 185(1):45–55, 2010.
- [36] A. Quarteroni, R. Sacco, and F. Saleri. *Numerical Mathematics*. Texts in Applied Mathematics. Springer, 2000.
- [37] E.L. Rees. Graphical discussion of the roots of a quartic equation. *The American Mathematical Monthly*, 29(2):51–55, 1922.
- [38] J.E. Rothenberg. Modulational instability for normal dispersion. *Phys. Rev. A*, 42:682–685, 1990.
- [39] J.E. Rothenberg. Observation of the buildup of modulational instability from wave breaking. *Opt. Lett.*, 16(1):18–20, 1991.
- [40] R.L. Sachs. Completeness of derivatives of squared Schrödinger eigenfunctions and explicit solutions of the linearized KdV equation. *SIAM J. Math. Anal.*, 14:674–683, 1983.
- [41] D.V. Skryabin and W.J. Firth. Modulational instability of bright solitary waves in incoherently coupled nonlinear Schrödinger equations. *Phys. Rev. E*, 60(1):1019–1029, 1999.
- [42] D. Wang and C.R. Menyuk. Polarization Evolution Due to the Kerr Nonlinearity and Chromatic Dispersion. *J. Lightwave Technol.*, 17(12):2520, 1999.
- [43] J. Yang. Complete eigenfunctions of linearized integrable equations expanded around a soliton solution. *J. Math. Phys.*, 41(9):6614–6638, 2000.
- [44] J. Yang. Eigenfunctions of linearized integrable equations expanded around an arbitrary solution. *Studies in Applied Mathematics*, 108:145–159, 2002.
- [45] J. Yang and D.J. Benney. Some properties of nonlinear wave systems. *Studies in Applied Mathematics*, 96(1):111–139, 1996.
- [46] J. Yang and D.J. Kaup. Squared eigenfunctions for the Sasa-Satsuma equation. *J. Math. Phys.*, 50:023504, 2009.
- [47] H.C. Yuen and B.M. Lake. Instabilities of waves on deep water. *Annual Review of Fluid Mechanics*, 12(1):303–334, 1980.

- [48] V.E. Zakharov and A.A. Gelash. Superregular solitonic solutions: a novel scenario of the nonlinear stage of Modulation Instability. *Theor. Math. Phys.*, 120(2):997–1008, 2013.
- [49] V.E. Zakharov and E.I. Shulmann. To the integrability of the system of two coupled nonlinear Schrödinger equations. *Physica D*, 4(2):270–274, 1982.
- [50] V.E. Zakharov and L.A. Ostrovsky. Modulation instability: The beginning. *Physica D*, 238:540–548, 2009.